AFFDL-TR-79-3077

LEVEL II

(2)

AD A073379

AEROELASTIC RESPONSE ANALYSIS OF TWO DIMENSIONAL, SINGLE AND TWO DEGREE OF FREEDOM AIRFOILS IN LOW-FREQUENCY, SMALL-DISTURBANCE UNSTEADY TRANSONIC FLOW

T. Y. Yang
P. Guruswamy
A. G. Striz

June 1979

Final Report November 1978 - May 1979

Approved for public release; distribution unlimited.

AIR FORCE FLIGHT DYNAMICS LABORATORY
AIR FORCE WRIGHT AERONAUTICAL LABORATORIES
AIR FORCE SYSTEMS COMMAND
WRIGHT-PATTERSON AIR FORCE BASE, OHIO 45433

DISCLAIMER NOTICE

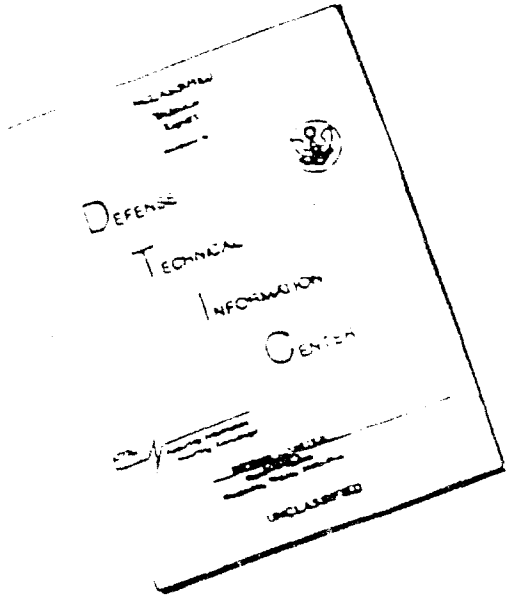

THIS DOCUMENT IS BEST QUALITY AVAILABLE. THE COPY FURNISHED TO DTIC CONTAINED A SIGNIFICANT NUMBER OF PAGES WHICH DO NOT REPRODUCE LEGIBLY.

NOTICE

When Government drawings, specifications, or other data are used for any purpose other than in connection with a definitely related Government procurement operation, the United States Government thereby incurs no responsibility nor any obligation whatsoever; and the fact that the government may have formulated, furnished, or in any way supplied the said drawings, specifications, or other data, is not to be regarded by implication or otherwise as in any manner licensing the holder or any other person or corporation, or conveying any rights or permission to manufacture, use, or sell any patented invention that may in any way be related thereto.

This report has been reviewed by the Information Office, (ASD/OIP) and is releasable to the National Technical Information Service (NTIS). At NTIS, it will be available to the general public, including foreign nations.

This technical report has been reviewed and is approved for publication.

Lawrence J. Huttsell

LAWRENCE J. HUTTSELL
Project Engineer
Aeroelastic Group
Analysis & Optimization Branch

Hartley M. Caldwell

HARTLEY M. CALDWELL, III, Capt, USAF
Actg, Ch, Analysis & Optimization Br
Structures & Dynamic Division

FOR THE COMMANDER

Ralph L Kuster Jr

RALPH L. KUSTER, Jr, Col, USAF
Chief, Structures & Dynamics Division

Copies of this report should not be returned unless return is required by security considerations, contractual obligations, or notice on a specific document.

Unclassified

SECURITY CLASSIFICATION OF THIS PAGE (When Data Entered)

REPORT DOCUMENTATION PAGE	READ INSTRUCTIONS BEFORE COMPLETING FORM
1. REPORT NUMBER: AFFDL-TR-79-3077	2. GOVT ACCESSION NO. / 3. RECIPIENT'S CATALOG NUMBER
4. TITLE (and Subtitle): AEROELASTIC RESPONSE ANALYSIS OF TWO DIMENSIONAL, SINGLE AND TWO DEGREE OF FREEDOM AIRFOILS IN LOW-FREQUENCY, SMALL-DISTURBANCE UNSTEADY TRANSONIC FLOW	5. TYPE OF REPORT & PERIOD COVERED: Technical Report, November 1978 - May 1979
	6. PERFORMING ORG. REPORT NUMBER
7. AUTHOR(s): T. Y. Yang, P. Guruswamy, A. G. Striz	8. CONTRACT OR GRANT NUMBER(s): AFOSR-78-3523A
9. PERFORMING ORGANIZATION NAME AND ADDRESS: School of Aeronautics and Astronautics, Purdue University, West Lafayette, IN 47907	10. PROGRAM ELEMENT, PROJECT, TASK AREA & WORK UNIT NUMBERS: PE 61102F, 2307/N5/11
11. CONTROLLING OFFICE NAME AND ADDRESS: Air Force Flight Dynamics Laboratory (FBR), Wright-Patterson AFB, OH 45433	12. REPORT DATE: Jun[illegible]79
	13. NUMBER OF PAGES: 65
14. MONITORING AGENCY NAME & ADDRESS (if different from Controlling Office)	15. SECURITY CLASS. (of this report): Unclassified
	15a. DECLASSIFICATION/DOWNGRADING SCHEDULE

16. DISTRIBUTION STATEMENT (of this Report)

Approved for public release; distribution unlimited.

17. DISTRIBUTION STATEMENT (of the abstract entered in Block 20, if different from Report)

18. SUPPLEMENTARY NOTES

19. KEY WORDS (Continue on reverse side if necessary and identify by block number)

Aeroelastic Response
Airfoils
Flutter
Transonic
Unsteady Aerodynamics

20. ABSTRACT (Continue on reverse side if necessary and identify by block number)

A procedure is developed to obtain the aeroelastic responses of single and two degree of freedom aeroelastic systems in transonic flow. The fluid is described by the two dimensional unsteady low-frequency transonic potential equation based on small disturbance theory. The aerodynamic computer code LTRAN2 which is based on a fully implicit time integration scheme is employed to obtain the aerodynamic forces. The structural equations are simultaneously integrated with the potential flow equations by a numerical method and the aeroelastic responses are obtained. Results for neutrally stable responses (cont

DD FORM 1 JAN 73 1473 EDITION OF 1 NOV 65 IS OBSOLETE

Unclassified

SECURITY CLASSIFICATION OF THIS PAGE (When Data Entered)

are compared with those obtained by the U-g method. Aeroelastic responses are obtained for flat plates (single and two degree of freedom) at M = 0.7 by the linear part of LTRAN2. Examples of an NACA 64A006 airfoil at Mach numbers of 0.88 and 0.85 are also analyzed. Response results obtained for a single pitching degree of freedom system at M = 0.88 are compared with an existing solution. The response results obtained for a two degree of freedom system at M = 0.85 for neutrally stable condition are correlated with those obtained by the flutter analysis. Results also include stable and unstable response curves and their variations with altitude.

FOREWORD

This report was prepared by Professor T. Y. Yang of the School of Aeronautics and Astronautics of Purdue University under AFOSR Grant 78-3523A, "Application of Time-Accurate Transonic Aerodynamics to Aeroelastic Problems." The research was administered by Lawrence J. Huttsell of the Structures and Dynamics Division, Air Force Flight Dynamics Laboratory, Wright-Patterson Air Force Base, Ohio.

The report covers work conducted from November 1978 to May 1979. T. Y. Yang was the principal investigator. Alfred G. Striz and P. Guruswamy were the graduate research assistants. Dr. Samuel R. Bland of NASA Langley Research Center and Dr. William F. Ballhaus of NASA Ames Research Center served as technical consultants.

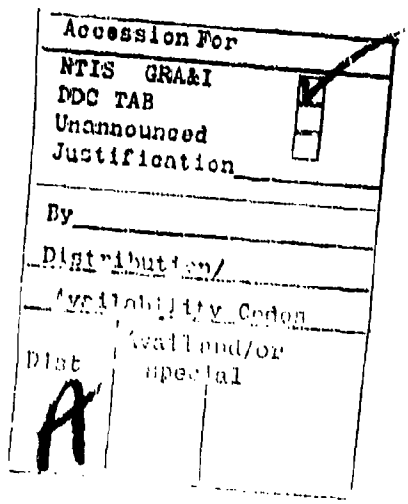

TABLE OF CONTENTS

LIST OF ILLUSTRATIONS

LIST OF ILLUSTRATIONS (continued)

LIST OF TABLES

LIST OF SYMBOLS

SYMBOL	DEFINITION
a_h	distance between midchord and elastic axis measured in semi-chords, positive towards the trailing edge
[A]	matrix of aerodynamic coefficients
A_1	$C_\alpha/I_\alpha\omega$, damping parameter for single degree of freedom pitching case
A_2	$K_\alpha/I_\alpha\omega^2$, stiffness parameter for single degree of freedom pitching case
A_3	$\pi/8\mu' k_c^2$, dynamic pressure parameter for single degree of freedom pitching case
b	half chord length of the airfoil
B_1	$C_h/m\omega$, damping parameter for single degree of freedom plunging case
B_2	$K_h/m\omega^2$, stiffness parameter for single degree of freedom plunging case
c	full chord length of the airfoil
[C]	mechanical damping coefficient matrix
C_h	mechanical damping coefficient corresponding to plunging
C_α	mechanical damping coefficient corresponding to pitching
c_ℓ	total aerodynamic lifting force coefficient
c_m	total aerodynamic moment coefficient about pitching axis
c_{ℓ_δ}	aerodynamic lifting force coefficient due to unit plunging displacement δ
c_{ℓ_α}	aerodynamic lifting force coefficient due to unit change in pitching angle α
c_{m_δ}	aerodynamic moment coefficient about pitching axis due to unit change in plunging displacement δ
c_{m_α}	aerodynamic moment coefficient about pitching axis due to unit change in pitching angle α
h	plunging degree of freedom positive when measured downwards
I_α	polar moment of inertia about elastic axis
k_b	$\omega b/U$, reduced frequency with respect to semi-chord length b
k_c	$\omega c/U$, reduced frequency with respect to full chord length c

LIST OF SYMBOLS (continued)

SYMBOL	DEFINITION
K_h	bending stiffness coefficient corresponding to plunging displacement
K_α	torsional stiffness coefficient corresponding to pitching rotation
[K]	matrix of stiffness coefficients
m	mass of the airfoil per unit span
M_∞	free stream Mach number
{p}	aerodynamic load vector
q	$\rho U^2/2$, dynamic pressure
Q_h	qcc_ℓ, total aerodynamic force
Q_α	qc^2c_m, total aerodynamic moment about pitching axis
r_α	$(I_\alpha/mb^2)^{1/2}$, radius of gyration about elastic axis in semi-chords
S	airfoil static moment about elastic axis
t	time in seconds
$\bar{t}$	ωt, nondimensional time parameter
{U}	displacement vector
U	free stream velocity
U^*	$U/b\omega_\alpha$, nondimensional flight speed parameter
x_α	S/mb, distance between the elastic axis and the mass center measured in semi-chords, positive towards the trailing edge
α	pitching degree of freedom measured positive in nose-up direction
α_i	induced angle of attack
β	$1/(1-M_\infty^2)^{1/2}$, Prandtl-Glauert number
γ	ratio of specific heats
δ	h/c
ζ_h	$C_h/m\omega$, uncoupled mechanical damping parameter corresponding to plunging in two degree of freedom system
ζ_α	$C_\alpha/mb^2\omega$, uncoupled mechanical damping parameter corresponding to pitching in two degree of freedom system
μ	$m/\pi\rho b^2$, airfoil-air mass ratio
μ'	$I_\alpha/\pi\rho b^4$, airfoil-air mass moment of inertia ratio

LIST OF SYMBOLS (continued)

SYMBOL	DEFINITION
ξ	h/b
ρ	free stream air density
τ	ratio of airfoil thickness to chord length
ϕ	disturbance velocity potential
ψ	phase angle between pitching moment and pitching angle
ω	flutter frequency of harmonic oscillation
ω_h	$(K_h/m)^{1/2}$, uncoupled plunging frequency of airfoil
ω_α	$(K_\alpha/I_\alpha)^{1/2}$, uncoupled torsional frequency of airfoil

SECTION I

INTRODUCTION

In the field of airplane design, there exists a class of problems in which the motion of an aeroelastic system may vary in an arbitrary manner with time, depending upon the initial conditions, the character of the applied forces, and dynamic response properties of the system. Rapidly applied external forces may rise from many sources during the life of a modern airplane. One of the most important disturbing forces is that produced by gusts. Detailed study of this phenomenon in subsonic, transonic and supersonic flows is important.

A time-dependent response study requires simultaneous integration of the structural and aerodynamic equations in time. In the subsonic and supersonic cases, the governing flow equations are linear and aerodynamic forces depend upon the body motion in a linear fashion. Many unsteady aerodynamic theories are available for the solution of the aeroelastic problems for these cases. Several classical examples, illustrating the dynamic response phenomena for the subsonic case may be found, for example, in Reference 1.

On the other hand, governing equations for flows in the transonic regime are nonlinear and they are characterized by the presence of shocks on the airfoil. Because of these complexities, the study of the aeroelastic phenomenon in the transonic regime is fairly involved. From earlier studies it has been observed that for the case of flow over an airfoil in a free stream at Mach numbers near one, small amplitude motions can cause large variations in the aerodynamic forces and moments. In addition, phase differences between the flow variables and the resultant forces may also be large. Because of these special characteristics of the transonic flows, the probability of encountering

aeroelastic instabilities is higher. Detailed investigations of this problem are of practical significance.

The numerical methods for the computation of aerodynamic forces of small-disturbance transonic flows about oscillating airfoils and planar wings have been rapidly developed in recent years. A brief mention of such developments containing 32 references can be found in Reference 2. Based on these developments many aeroelastic computations have been carried out. A comprehensive state-of-the-art review of the developments in transonic aeroelasticity is given by Ashley in Reference 3.

The first significant application of unsteady transonic computations to an aeroelastic response study was by Ballhaus and Goorjian (Reference 4). In that study they illustrated the use of the time-integration and the indicial approaches for the aeroelastic response problems. They performed an aeroelastic response analysis for a NACA 64A006 airfoil with a single pitching degree of freedom. Pitching axis was assumed to be at the mid-chord. The time-history responses were computed by using their computer program LTRAN2 for unsteady transonic flow coupled with an integration procedure for the simple differential equation of motion for the airfoil. The motion of the airfoil in a flow at $M_\infty = 0.88$ was forced for the first few cycles with an amplitude of oscillation of 0.5 degrees until the pitching moment became periodic, after which the airfoil motion and the aerodynamic response were left free to drive each other. As the structural damping coefficient was varied parametrically the responses were obtained for the highly damped, neutral, slightly divergent, and highly divergent cases. It was shown that in order to obtain a flutter solution for their example system at $M_\infty \geq 0.88$, it is necessary that the nonlinear aerodynamic equations be used and that the moment variation lead the motion. Here it may be noted that linear flat plate equations can not be used to predict a phase lead and can not be used to obtain a flutter solution.

In Reference 4 another case with large initial amplitude of 1.5^{0} and $M_{\infty} = 0.87$ was also considered. This example illustrated a non-sinusoidal pitching moment behavior that could result from the large shock wave excursions encountered at larger airfoil motion amplitudes.

In Reference 5, Rizzetta performed an aeroelastic response study of a NACA 64A010 airfoil by simultaneously integrating the LTRAN2 aerodynamics program and the structural equations of motion. The study included a single degree of freedom case with airfoil pitching at quarter chord and a three degree of freedom case with airfoil pitching, plunging, and aileron pitching.

Mach numbers considered in Reference 5 were 0.72 and 0.82. A procedure similar to that discussed in Reference 4 was employed to analyze the single pitching degree of freedom case. For the three degree of freedom case, results were obtained as plots of nondimensional pitching displacement (and moment), plunging displacement (and lift) and aileron displacement (and moment)versus time for various arbitrary values of the airfoil-air mass ratios. The other aeroelastic parameters were also selected arbitrarily. All the displacement and force quantities in the figures were divided by $\alpha'(0)$, the initial pitching velocity. Dimensional values for $\alpha'(0)$ corresponded to 1,3, and 5 degrees. By varying the values of μ, converging and diverging curves were obtained.

It was pointed out in Reference 5 that no attempt was made to obtain response curves corresponding to flutter condition for the three degree of freedom system. The accuracy of results was tested against the homogeneous solutions obtained for the structural system without the aerodynamic forces. It was achieved by assuming large values for μ. At large values of μ the quantities in the aerodynamic matrix have negligible effect on the response solution.

The aeroelastic response studies made in the transonic regime so far have not included the single degree of freedom case of airfoil plunging and the two

degree of freedom case with airfoil pitching and plunging. Although the single degree of freedom systems do not represent the "real world" problems, some studies of them may give insight to other practical aeroelastic problems. On the other hand the earlier studies have shown that primary flexure-torsion flutter corresponding to the two degree of freedom system is the most destructive of all aeroelastic instabilities. The "transonic dip" phenomenon reported in References 6,7 and 8 showed that flexure-torsion flutter may be more hazardous at Mach numbers near one. Studies conducted so far (References 2,3,6,7,9) included only the results corresponding to the neutral stability (flutter) point for transonic Mach numbers. The response studies in the neighborhood of these transonic neutral stability points are also of significant interest.

In this study aeroelastic response analyses were performed for a flat plate and a NACA 64A006 airfoil. Several cases with single degree of freedom of pitching, single degree of freedom of plunging, and two degrees of freedom of pitching and plunging were considered in detail. Aerodynamic forces required in this analysis were obtained by time-integration method with the use of the LTRAN2 computer code.

To evaluate the linear solution obtained by using LTRAN2, a flat plate was first analyzed at $M_\infty = 0.7$. Converging type response was obtained for a flat plate pitching at mid-chord by simultaneously integrating LTRAN2 with the corresponding structural equation of motion. For the same case, response was also obtained by integrating the aerodynamic equation given by the quasi steady-state theory with the structural equation of motion. Responses for pitching angle and pitching moment were obtained by using both methods and the two sets of results were compared with each other.

An example identical to that discussed in Reference 4 was also considered. In the example a NACA 64A006 airfoil with single degree of freedom pitching

about mid-chord at $M_\infty = 0.88$ was considered. In this study the aerodynamic coefficients required for the analysis were obtained by time integration method, whereas in Reference 4 the indicial method was employed to obtain the same aerodynamic coefficients. Response results obtained from both studies for neutrally stable, diverging, and converging cases are compared and discussed. This example was also used to evaluate the numerical integration scheme employed in the present analysis.

Another case of a single plunging degree of freedom system for a flat plate at Mach number of 0.7 was also considered. Converging type plunging response results were obtained by using both the aerodynamic forces computed by LTRAN2 and quasi steady-state aerodynamic theory. The two sets of results were compared.

Finally, the important case of a two degree of freedom system with plunging and pitching was analyzed. Two configurations, one in the form of a flat plate and the other a NACA 64A006 airfoil were considered.

The flat plate was assumed to pitch about the mid-chord at $M_\infty = 0.7$. Flutter speeds and corresponding reduced frequencies were first obtained by varying the airfoil-air mass ratio μ for selected values of plunge to pitch frequency ratio ω_h/ω_α, position of mass center x_α, and radius of gyration r_α. The aerodynamic coefficients required for this analysis were obtained by both LTRAN2 (linear) and a Kernel Function method. For a selected point on the flutter curve (say, a point corresponding to reduced frequency $k_c = 0.1$) a response study was carried out. Neutrally stable, stable and unstable response results in the form of displacements and forces were obtained by varying the airfoil-air mass ratio μ. These results are discussed. The effect of airfoil-air mass ratio on peak amplitudes was also studied.

A study similar to that performed for a flat plate was also carried out for a NACA 64A006 airfoil pitching about the quarter chord at $M = 0.85$. The

plots of flutter speeds and the corresponding reduced frequencies versus airfoil-air mass ratio μ were obtained by using the aerodynamic coefficients computed by time integration method. These results were compared with those obtained by using relaxation and indicial methods in Reference 2. For a selected point on these flutter curves, a response study was carried out. Neutrally stable, stable and unstable response results were obtained in the form of displacements and forces by varying the airfoil-air mass ratio μ. These results are discussed. The effect of airfoil-air mass ratio μ on peak amplitudes was also studied for the NACA 64A006.

SECTION II

GOVERNING AERODYNAMIC AND AEROELASTIC EQUATIONS OF MOTION

In this section the basic equations employed in the present work both for the aerodynamic part and structural part of the equations of motion are discussed.

2.1 Transonic Flow Equations

Many numerical procedures have been developed for computations of transonic unsteady flow fields around oscillating two-dimensional airfoils. A brief description of these developments is given in Reference 2. In this report the time integration method developed by Ballhaus and Goorjian (Reference 8) is used.

The simplified basic aerodynamic equations, following the assumptions that the flow is two-dimensional, inviscid, transonic ($M_\infty \approx 1$), and that the velocity disturbances are small as compared to the free stream velocity U, can be deduced from the general equation of continuity of gas dynamics as

$$k_c^2 M_\infty^2 \phi_{tt} + 2k_c M_\infty^2 \phi_{xt} = V_c \phi_{xx} + \phi_{yy} \qquad (1)$$

where $k_c = \omega c/U$ is the reduced frequency; M_∞ is the free stream Mach number; ϕ is the disturbance velocity potential; $V_c = 1 - M_\infty^2 - (\gamma+1)M_\infty^m \phi_x$; m is a function of M_∞; and γ is the ratio of specific heats.

In deriving the above equation, the coordinate system is fixed with respect to the airfoil, and x is aligned with the free stream direction. The flow is defined as locally subsonic or supersonic, relative to the fixed coordinate system, for $V_c > 0$ or $V_c < 0$, respectively. A measure of the degree of unsteadiness is given by the reduced frequency k_c when the airfoil is oscillating periodically with a frequency ω in rad/sec.

As a further simplification of Equation 1, the frequency of the transonic flow can be assumed as low so that $k_c \approx 1 - M_\infty^2 \approx \tau^{2/3} \ll 1$. Equation 1 may then be reduced to

$$2k_c M_\infty^2 \phi_{xt} = V_c \phi_{xx} + \phi_{yy} \qquad (2)$$

where τ is the thickness-chord ratio of the airfoil.

Equation 2 is suitable for the time integration approach. This approach is based on the finite difference scheme that integrates Equation 2 in time for harmonic aerodynamic motions until the transient states in the solution disappear and the forces become periodic.

Several numerical procedures are available to solve Equation 2. Among them the procedure developed by Ballhaus and Goorjian (Reference 10) based on the alternate-direction implicit algorithm has been proven to be computationally efficient and is being widely used. This procedure uses a conservative, implicit finite-difference scheme to time-accurately integrate the nonlinear, low-frequency transonic small-disturbance equation as defined in Equation 2. A computer code LTRAN2 was developed based on this procedure. This code can be used to find the flow field solutions for the airfoils with arbitrary combinations of pitch, plunge and flap deflections.

2.2 Quasi Steady-State Aerodynamic Equations for Flat Plates

For subsonic flow conditions exact unsteady aerodynamic solutions are available for flat plates with arbitrary pitch and plunge motions. Depending upon certain assumptions these solutions may further be simplified. One such solution can be obtained by using quasi steady-state assumption.

Quasi steady-state theory neglects the influence of wake vortices on the flow. This is valid when the flat plate is oscillating with a very low reduced frequency ($k_c \approx 0.0$).

For a flat plate pitching with an angle α about an axis located at a distance ba_h from the mid-chord and plunging with displacement h, the expressions for quasi steady aerodynamic lifting force, Q_h, and moment, Q_α are given as (see chapter 5 of Reference 1),

$$Q_h = -\pi\rho b^2[\ddot{h} + U\dot{\alpha} - ba_h\ddot{\alpha}] - 2\pi\rho Ub[\dot{h} + U\alpha + b(1/2-a_h)\dot{\alpha}] \quad (3)$$

$$Q_\alpha = \pi\rho b^2[ba_h\ddot{h} - Ub(1/2 - a_h)\dot{\alpha} - b^2(1/8 + a_h^2)\ddot{\alpha}] \quad (4)$$
$$+ 2\pi\rho Ub^2(a_h + 1/2)[\dot{h} + U\alpha + b(1/2 - a_h)\dot{\alpha}]$$

where ba_h = distance of the pitching axis measured from mid-chord in semi-chords

b = semi-chord length of the airfoil.

The above equations are derived assuming that the flow is incompressible ($M_\infty = 0$). The effect of Mach number is approximated by multiplying the aerodynamic forces by the Prandtl-Glauert number, β, which is defined as

$$\beta = \frac{1}{\sqrt{1-M_\infty^2}} \quad (5)$$

In the present work it is assumed that the above equations are valid for flat plates oscillating at $M_\infty = 0.7$ with reduced frequency $k_c = 0.1$.

2.3 Aeroelastic Equations of Motion for Single and Two Degree of Freedom Airfoil System

In the present work two-dimensional airfoils in transonic flow with single pitching degree of freedom, single plunging degree of freedom and two degrees of freedom, plunge and pitch, are considered. Figure 1 describes the sign conventions and the variables used in this study.

2.3.1 Pitching Degree of Freedom System

The equation of motion for the case assuming that airfoil is pitching about an axis located at a distance $a_h b$ from the mid-chord, is

$$I_\alpha \ddot{\alpha} + C_\alpha \dot{\alpha} + K_\alpha \alpha = Q_\alpha \tag{6}$$

where I_α = mass moment of inertia of the airfoil about the elastic axis; K_α = spring constant corresponding to pitching; C_α = mechanical damping coefficient corresponding to pitching; Q_α is the aerodynamic moment about the pitching axis, defined positive in positive α direction.

A nondimensional form of Equation 3 can be written as

$$\alpha'' + A_1 \alpha' + A_2 \alpha = \frac{Q_\alpha}{I_\alpha \omega^2} \tag{7}$$

where the prime represents the differentiation with respect to nondimensional time ωt and ω is the circular frequency of oscillation. $A_1 = C_\alpha / I_\alpha \omega$ and $A_2 = K_\alpha / I_\alpha \omega^2$ are the nondimensional damping and stiffness parameters, respectively.

The aerodynamic moment Q_α may be written as

$$Q_\alpha = qc^2 c_m \tag{8}$$

where $q = 1/2 \rho U^2$, dynamic pressure

c = full chord length of the airfoil

ρ = free stream density

c_m = aerodynamic moment coefficient.

The values for c_m are computed from LTRAN2.

Using Equation 8 and the definition $k_c = \omega c / U$, Equation 7 can be rewritten as

$$\alpha'' + A_1 \alpha' + A_2 \alpha = \frac{8}{\pi \mu' k_c^2} c_m \tag{9}$$

This equation is incorporated in LTRAN2 to obtain the aeroelastic responses.

The following derivations are based on the assumption that Q_α is obtained from quasi steady-state aerodynamic theory.

For a single pitching degree of freedom system, the aerodynamic moment Q_α for the two degree of freedom case as given in Equation 4 may be reduced to the form

$$Q_\alpha = \pi\rho b^2(-Ub(1/2 - a_h)\dot{\alpha} - b^2(1/8 + a_h^2)\ddot{\alpha})$$

$$+ 2\pi\rho Ub^2(a_h + 1/2)(U\alpha + b(0.5 - a_h)\dot{\alpha}) \qquad (10)$$

Correcting this Q_α for the effect of Mach number and substituting it into Equation 7 give

$$d_1\alpha'' + e_1\alpha' + f_1\alpha = 0 \qquad (11)$$

where $$d_1 = 1.0 + \frac{(0.125+a_h^2)\beta}{\mu'}$$

$$e_1 = A_1 + \frac{2(0.5-a_h)\beta}{\mu' k_c} + \frac{4(a_h^2-0.25)\beta}{\mu' k_c}$$

$$f_1 = A_2 - \frac{8(a_h+0.5)\beta}{\mu' k_c^2}$$

$\mu' = \frac{I_\alpha}{\pi\rho b^4}$, airfoil-air mass moment of inertia ratio.

Equation 11 is a second order, ordinary differential equation. From this equation the closed form solution for pitching response can be obtained for given initial conditions and other variables.

2.3.2 Plunging Degree of Freedom System

If h is the plunging displacement measured positive downwards from a mean position, the equation of motion for the system can be written as

$$m\ddot{h} + C_h\dot{h} + K_h h = Q_h \qquad (12)$$

where m = mass of the airfoil per unit span; C_h = damping coefficient corresponding to plunging; K_h = spring constant corresponding to plunging; and Q_h = aerodynamic lifting force defined positive in positive h direction.

The nondimensional form of Equation 12 is written as

$$\delta'' + B_1\delta' + B_2\delta = \frac{Q_h}{m\omega^2 c} \qquad (13)$$

where the prime represents the derivative with respect to nondimensional time ωt; $\delta = h/c$, nondimensional plunging displacement; $B_1 = C_h/m\omega$, nondimensional damping parameter; $B_2 = K_h/m\omega^2$, nondimensional stiffness parameter.

The aerodynamic force Q_h may be expressed as

$$Q_h = - qcc_\ell \tag{14}$$

where c_ℓ is the lift coefficient which can be obtained by LTRAN2. A negative sign is introduced in Equation 14 since lift force is defined positive upwards in the computer code.

Substituting Equation 14 in Equation 13 and rearranging give

$$\delta'' + B_1\delta' + B_2\delta = - \frac{2c_\ell}{\pi\mu k_c^2} \tag{15}$$

where $\mu = \frac{m}{\pi\rho b^2}$, airfoil-air mass ratio

This equation is incorporated in the LTRAN2 code to obtain the aeroelastic responses for the plunging case.

The following derivations are based on the assumption that an explicit expression for Q_h is obtainable from the quasi steady-state aerodynamic theory. For a single plunging degree of freedom system, the aerodynamic force Q_h for (Equation 3) may be written as

$$Q_h = - 2\pi U\rho b\dot{h} - \pi\rho b^2\ddot{h} \tag{16}$$

Correcting the Q_h for the effect of Mach number and substituting it into Equation 13 give

$$d_2\delta'' + e_2\delta' + f_2\delta = 0 \tag{17}$$

where $d_2 = 1 + \frac{\beta}{\mu}$, $e_2 = B_1 + \frac{4\beta}{\mu k_c}$, $f_2 = B_2$

Equation 17 is a second order ordinary differential equation. From this equation, closed form solutions can be obtained for plunging responses for given initial conditions and other variables.

2.3.3 Two Dimensional Airfoil with Pitch and Plunge Degrees of Freedom

Figure 1 shows an airfoil plunging with a positive displacement h (downward) and pitching with a positive angle α (with the nose up) about elastic axis. The elastic axis is located at a distance $a_h b$ from the mid-chord while the mass center is located at a distance $x_\alpha b$ from the elastic axis. Both distances are defined positive when measured toward the trailing edge.

In this analysis it is assumed that the airfoil is rigid and the amplitudes of oscillation are small. It is also assumed that there is no coupling in the mechanical damping. Hence considering the inertia forces, damping forces, elastic forces, and aerodynamic forces, the equations of motion are

$$m\ddot{h} + S\ddot{\alpha} + C_h\dot{h} + K_h h = Q_h \tag{18a}$$

$$S\ddot{h} + I_\alpha\ddot{\alpha} + C_\alpha\dot{\alpha} + K_\alpha\alpha = Q_\alpha \tag{18b}$$

where S = airfoil static moment about the elastic axis and other quantities have the same definitions as given in the single degree of freedom system.

The nondimensional form of Equation 18 can be written as

$$\xi'' + x_\alpha\alpha'' + \zeta_h\xi' + \left(\frac{\omega_h}{\omega}\right)^2\xi = \frac{Q_h}{mb\omega^2} \tag{19a}$$

$$x_\alpha\xi'' + r_\alpha^2\alpha'' + \zeta_\alpha\alpha' + r_\alpha^2\left(\frac{\omega_\alpha}{\omega}\right)^2\alpha = \frac{Q_\alpha}{mb^2\omega^2} \tag{19b}$$

where the prime represents the derivative with respect to nondimensional time ωt; $\xi = h/b$ is nondimensional plunging displacement; $x_\alpha = S/mb$ is a coefficient to be multiplied by the semi-chord length to locate the mass center from the elastic axis; $\omega_h = (K_h/m)^{1/2}$ is the uncoupled plunging frequency; ω is the frequency of oscillation of the system; $r_\alpha = (I_\alpha/mb^2)^{1/2}$ is the coefficient to be multiplied by the semi-chord to give the radius of gyration about the elastic axis; $\omega_\alpha = (K_\alpha/I_\alpha)^{\frac{1}{2}}$ is the uncoupled pitching frequency; $\zeta_h = (C_h/m\omega)$ is the nondimensional damping

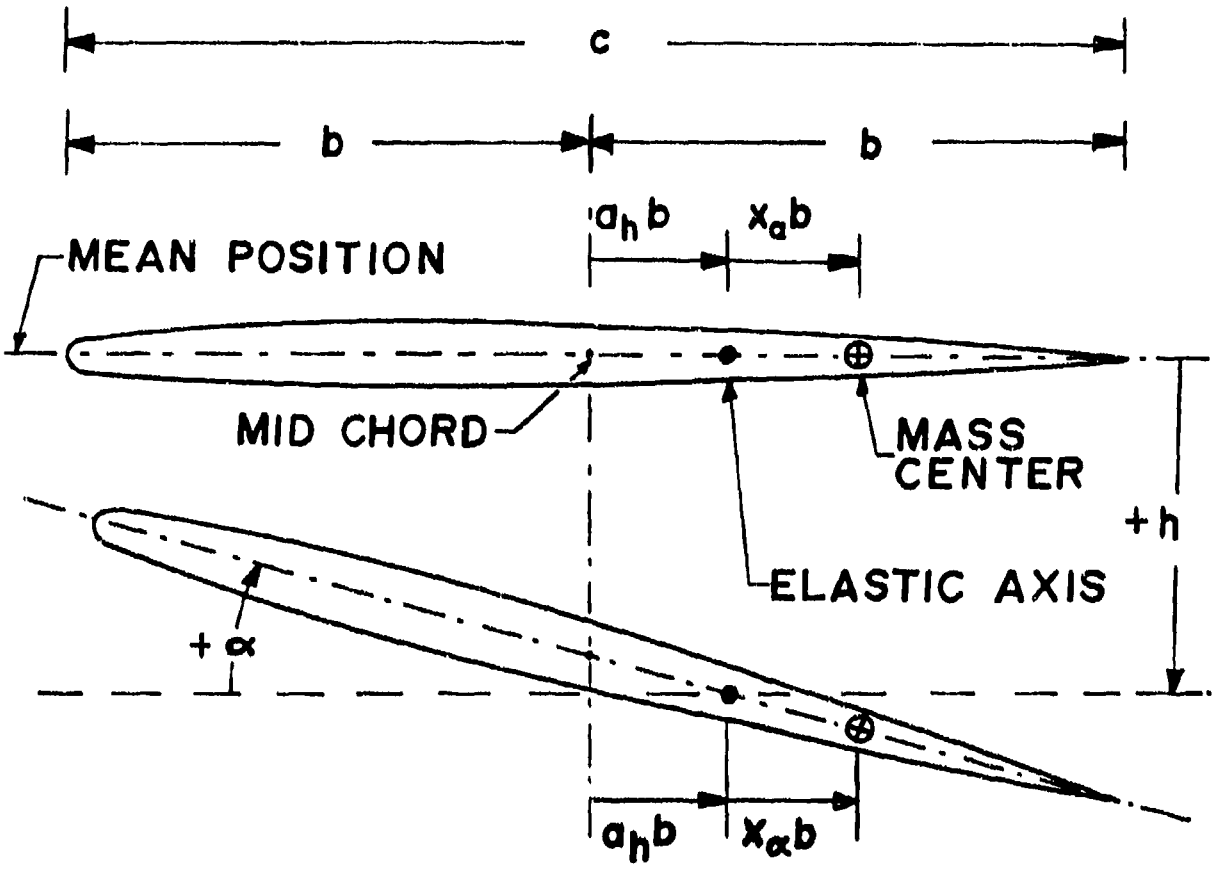

Figure 1. Definition of Parameters for Two Degree of Freedom Aeroelastic Analysis

parameter corresponding to plunging; $\zeta_\alpha = (C_\alpha/mb^2\omega)$ is the nondimensional damping parameter corresponding to pitching.

Substituting Equations 8 and 14 into Equation 19 and rearranging, the final matrix equation for the response analyses is

$$[M]\begin{Bmatrix}\xi'' \\ \alpha''\end{Bmatrix} + [C]\begin{Bmatrix}\xi' \\ \alpha'\end{Bmatrix} + [K]\begin{Bmatrix}\xi \\ \alpha\end{Bmatrix} = \frac{4}{\pi\mu k_c^2}\begin{Bmatrix}-c_\ell \\ 2c_m\end{Bmatrix} \tag{20}$$

where [M], [C], and [K] are the mass, damping and stiffness matrices, respectively, and they are defined as

$$[M] = \begin{bmatrix} 1 & x_\alpha \\ x_\alpha & r_\alpha^2 \end{bmatrix} \tag{21a}$$

$$[C] = \begin{bmatrix} \zeta_h & 0 \\ 0 & \zeta_\alpha \end{bmatrix} \tag{21b}$$

$$[K] = \left(\frac{2}{U^* k_c}\right)^2 \begin{bmatrix} (\omega_h/\omega_\alpha)^2 & 0 \\ 0 & r_\alpha^2 \end{bmatrix} \tag{21c}$$

where $U^* = U/b\omega_\alpha$ is the nondimensional flight speed parameter and c_ℓ and c_m are the aerodynamic lifting and moment coefficients. These quantities are directly obtained from the computer program LTRAN2.

Equation 20 is incorporated into LTRAN2 to obtain the aeroelastic responses for two dimensional airfoils with pitching and plunging degrees of freedom.

SECTION III

RESPONSE SOLUTION PROCEDURE

In order to obtain the aeroelastic response solutions it is necessary to simulataneously integrate the structural and aerodynamic equations. In the present analysis this integration is carried out by a numerical procedure.

3.1 Direct Integration Method

The aeroelastic Equations 9, 15, and 20 can be written in a general form as

$$[M]\{u''\} + [C]\{u'\} + [K]\{u\} = \{p\} \tag{22}$$

where [M], [C], and [K] are the mass, damping, and stiffness matrices, respectively; {u} is the vector of the displacement degrees of freedom for the structure; prime denotes the derivatives with respect to nondimensional time $\bar{t} = \omega t$; {p} is the vector of the aerodynamic loads. Equation 22 is in the form suited for numerical integration.

Many numerical procedures are available in the literature for the solution of the equations of motion in a form similar to Equation 22. Discussion of such procedures as applied to dynamic problems of structures can be found in references, such as 11. In the present analysis the common direct integration procedure is employed to find the time-history dynamic responses of the aeroelastic system. The solution is obtained by using a step-by-step time integration finite difference approach.

Assuming a linear variation of acceleration, the velocities and displacements at the end of a small time interval $\Delta\bar{t}$ can be expressed as

$$\{u'\}_{\bar{t}} = \{u'\}_{\bar{t}-\Delta\bar{t}} + \frac{\Delta\bar{t}}{2}\{u''\}_{\bar{t}-\Delta\bar{t}} + \frac{\Delta\bar{t}}{2}\{u''\}_{\bar{t}} \tag{23a}$$

$$\{u\}_{\bar{t}} = \{u\}_{\bar{t}-\Delta\bar{t}} + \Delta\bar{t}\{u'\}_{\bar{t}-\Delta\bar{t}} + \frac{\Delta\bar{t}^2}{3}\{u''\}_{\bar{t}-\Delta\bar{t}} + \frac{\Delta\bar{t}^2}{6}\{u''\}_{\bar{t}} \tag{23b}$$

Substituting Equations 23a and 23b into 22 yields

$$\{u''\}_{\bar{t}} = [F]\left[\{p\}_{\bar{t}} - [C]\{v\} - [K]\{w\}\right] \tag{24}$$

where

$$[F] = \left[[M] + \frac{\Delta\bar{t}}{2}[C] + \frac{\Delta\bar{t}^2}{6}[K]\right]^{-1} \tag{25a}$$

$$\{v\} = \{u'\}_{\bar{t}-\Delta\bar{t}} + \frac{\Delta\bar{t}}{2}\{u''\}_{\bar{t}-\Delta\bar{t}} \tag{25b}$$

$$\{w\} = \{u\}_{\bar{t}-\Delta\bar{t}} + \Delta\bar{t}\{u'\}_{\bar{t}-\Delta\bar{t}} + \frac{\Delta\bar{t}^2}{3}\{u''\}_{\bar{t}-\Delta\bar{t}} \tag{25c}$$

For small amplitude (structurally linear) problems, matrix [F] need only be formed once since it is independent of time. On the other hand the aerodynamic load vector {p} depends upon the displacement degrees of freedom {u}, the time derivatives of {u}, the reduced frequency k_c and the free stream Mach number M_∞. The vector {p} is obtained by numerically solving the transonic aerodynamic Equation 2 with the use of LTRAN2. The values of {u} and the time derivatives of {u} used for computing {p} are based on the values obtained at the time $\bar{t}-\Delta\bar{t}$.

3.2 Solution for Aerodynamic Forces {p} by LTRAN2

The basic LTRAN2 code employs a non-iterative alternating direction implicit (ADI) scheme to advance the solution for the perturbation potential, ϕ, from one time interval to the next at each grid point in the computational flow field. Differencing in x-direction is of mixed type which has been quite successful in maintaining stability for both subsonic and supersonic flow regions. The conservative form of the equation is preserved, which is essential for the proper description of the shock wave motions. While the ADI scheme has no time step limitation for stability based on classical linear stability analysis, instabilities may be generated by the motion of shock waves due to the mixed differencing. Hence, the time interval $\Delta\bar{t}$ must be chosen such that shock waves do not travel more than one mesh point in the x-direction over a single time step. Based on this procedure pressure distributions at any time can be computed.

By integrating these pressure curves, aerodynamic lifting forces and moments are computed.

At every time step LTRAN2 requires the effective induced angle of attack α_i and its time derivatives as input. In general, for the two degree of freedom system described in Figure 1 the induced angle of attack α_i can be defined as

$$\alpha_i = \alpha + \frac{\dot{h}}{U} \tag{26a}$$

or

$$\alpha_i = \alpha + \frac{k_c}{2} \xi' \tag{26b}$$

α and ξ' at every time step can be computed from the direct integration scheme discussed earlier in this section.

3.3 Summary of Step by Step Time Integration of Aeroelastic Equations

The procedure discussed in this section was incorporated in LTRAN2 in the following manner. For a set of starting values of {u}, {u'}, and {p}, (say, known at time $\bar{t}-\Delta\bar{t}$) the acceleration vector {u"} at time $\bar{t}$ was computed from Equation 24. Based on the known acceleration vector {u"}, the displacement vector {u} and velocity vector {u'} at time $\bar{t}$ were computed from Equations 23a and 23b, respectively. From these quantities the effective induced angle of attack α_i, and its time derivatives were computed for time $\bar{t}$. This induced angle of attack α_i and other required quantities were then read into the LTRAN2 code and the new aerodynamic load vector {p} at time $\bar{t}$ was computed. At this stage all the quantities, namely, {u}, {u'}, {u"}, and {p} at time $\bar{t}$ were known so that further computations for time $\bar{t} + \Delta\bar{t}$ can be carried out. This process was repeated for every time step.

SECTION IV

RESULTS

Aeroelastic response analyses were carried out for two airfoil configurations, a flat plate and a NACA 64A006 airfoil. In both cases, the airfoils were considered as single and two degree of freedom systems.

4.1 Finite Difference Computational Grid

The size and the pattern of the grid play an important role in obtaining accurate results from LTRAN2. Because of the various reasons discussed in Reference 10, a fairly fine mesh is required in order to obtain acceptable solutions. However, the mesh size is limited by the capacity of the core memory availalbe in a computer.

In this analysis a 79 x 99 finite difference mesh, with 79 grid points in the vertical (y) direction and 99 grid points in horizontal (x) direction, was employed for final computations. Details of this grid were kindly supplied by Ballhaus and Goorjian. This was the maximum grid size that could be practically used on the CDC 6500 computer available at Purdue University. A schematic diagram of the portion of the grid near the airfoil is shown in Figure 2.

This grid has a smooth non-uniform pattern and it is symmetric about the $y = 0$ line. The spacings of the grid points are smaller near the leading and trailing edges in x-direction and near the mean chord line in the y-direction. The spacings are gradually enlarged as the grid points are farther away from the airfoil. Thus the grid boundaries are located sufficiently away from the airfoil both in x-and y-directions. From leading edge to trailing edge, a total of 33 grid points is used so that an accurate representation of the pressure distribution can be obtained, particularly when there is a shock. Other salient features for this grid are given as follows:

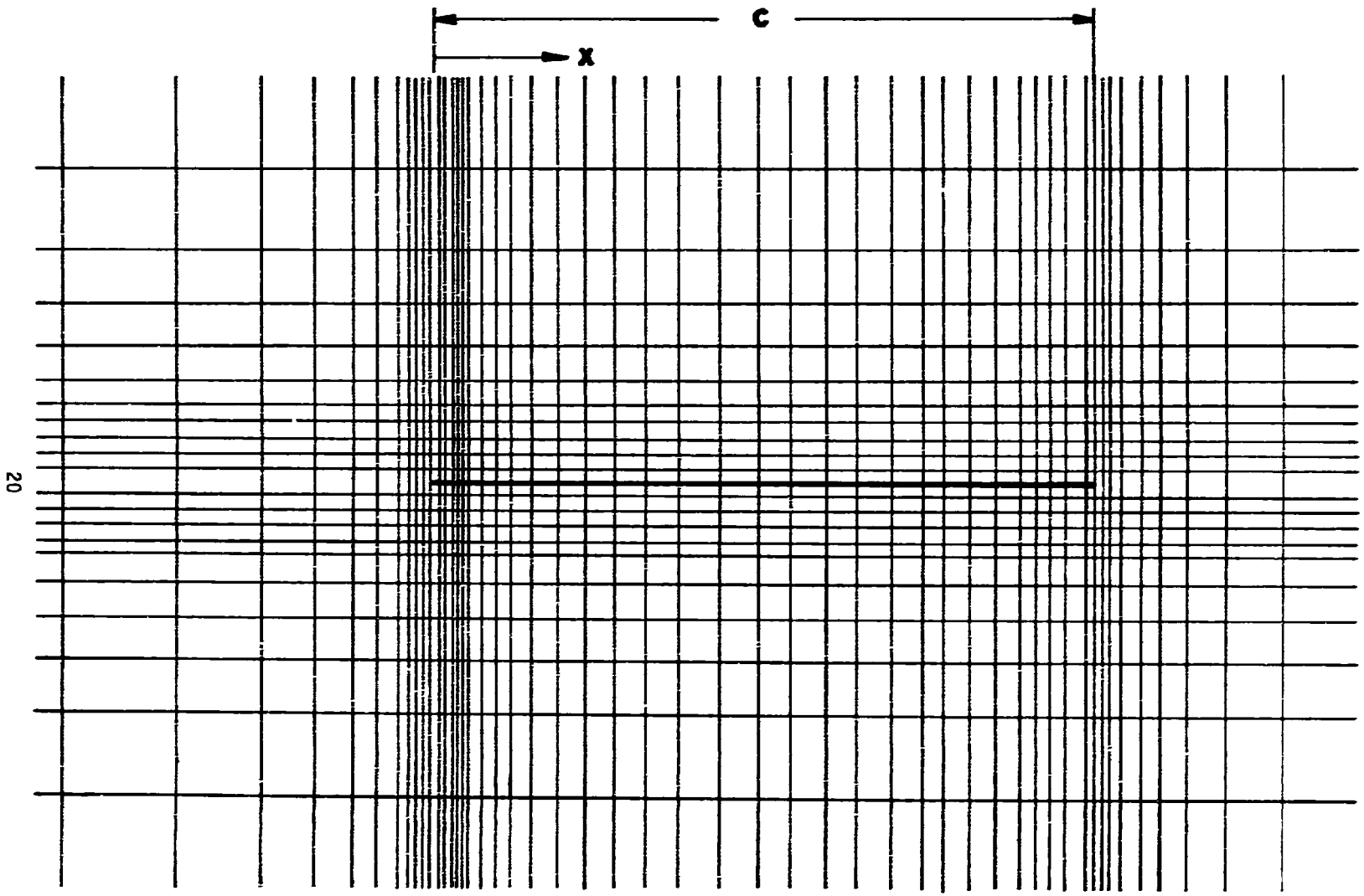

Figure 2. Computational Mesh near Airfoil

(1) Minimum spacing in x-direction = 0.0033c

(2) Minimum spacing in y-direction = 0.02c

(3) Distance between the upstream grid boundary and the leading edge = 1033.53c

(4) Distance between the downstream grid boundary and the leading edge = 855.91c

(5) Distance between grid boundary and the mean chord line = 811.12c.

4.2 Steady-State Computations

The steady-state solution is required as an initial condition for the unsteady computations. In this analysis the steady-state solution was obtained by using the successive line over-relaxation method (SLOR) available in the LTRAN2 code.

In the process of obtaining the steady-state solution, multiple grid computations were carried out in order to accelerate the rate of convergence. First, a converged steady-state solution was obtained for a coarse grid (35x38). This solution was then interpolated to form a starting solution for a medium grid (53x79). A converged solution was then obtained for the medium grid. This solution was again interpolated to form a starting solution for the final computational grid (79 x 99).

The SLOR computations were carried out for the fine grid (79x99) for several hundred iterations. This iterative process was stopped when the variation in the perturbation velocity potential at all grid points between consecutive iterations reached a value of about 4×10^{-5}. This required about 600 iterations. The steady solution obtained at this stage was used to plot the pressure curves and also used as a starting solution for the unsteady computations.

4.3 Unsteady Computations (Forced Motion)

Steady-state results obtained by the SLOR method were used as the initial conditions for unsteady computations. In order to obtain unsteady results the

airfoil was first subjected to a harmonic forced motion. In most of the cases the induced angle of attack α_1 was varied sinusoidally with an amplitude of 0.01 radians(0.574^0) and Equation 2 was integrated in time by LTRAN2. During the process of time integration, 120 time steps per cycle were used. After some duration of time the effect of the initial conditions on the unsteady solution became negligible such that the aerodynamic force coefficients c_ℓ and c_m became periodic. In general, four to six cycles of forced motion were required to obtain fairly periodic results from LTRAN2. However, the exact time at which the forced motion had to be stopped, depended upon the type of initial conditions specified for free motion. For all the cases studied, forced motion was stopped such that α_1, α_1', and α_1'' were 0.0, 0.01, and 0.0, respectively, with α_1 in the unit of radians. From this stage onwards free motion conditions were simulated by simultaneously integrating the structural and aerodynamic equations and allowing the airfoil motion and aerodynamic response to drive each other.

Due to inherent nonlinearity in the transonic aerodynamic equation, the free motion response solution depends upon the initial values for α_1, α_1', and α_1''. Physically these initial conditions may be used to represent the impulsive forces (gusts) striking the airfoil.

4.4 Response Analysis of Single Degree of Freedom Systems

4.4.1 NACA 64A006 Airfoil Pitching at M = 0.88

A case of a NACA 64A006 airfoil pitching about the mid-chord at $M_\infty = 0.88$ and $k_c = 0.1$ was considered. This case was selected in order to verify the present formulations and also compare the results with those already obtained by Ballhaus and Goorjian (Reference 4).

The airfoil configuration data required for this case were obtained from Reference 12. The airfoil configuration is shown in Figure 3.

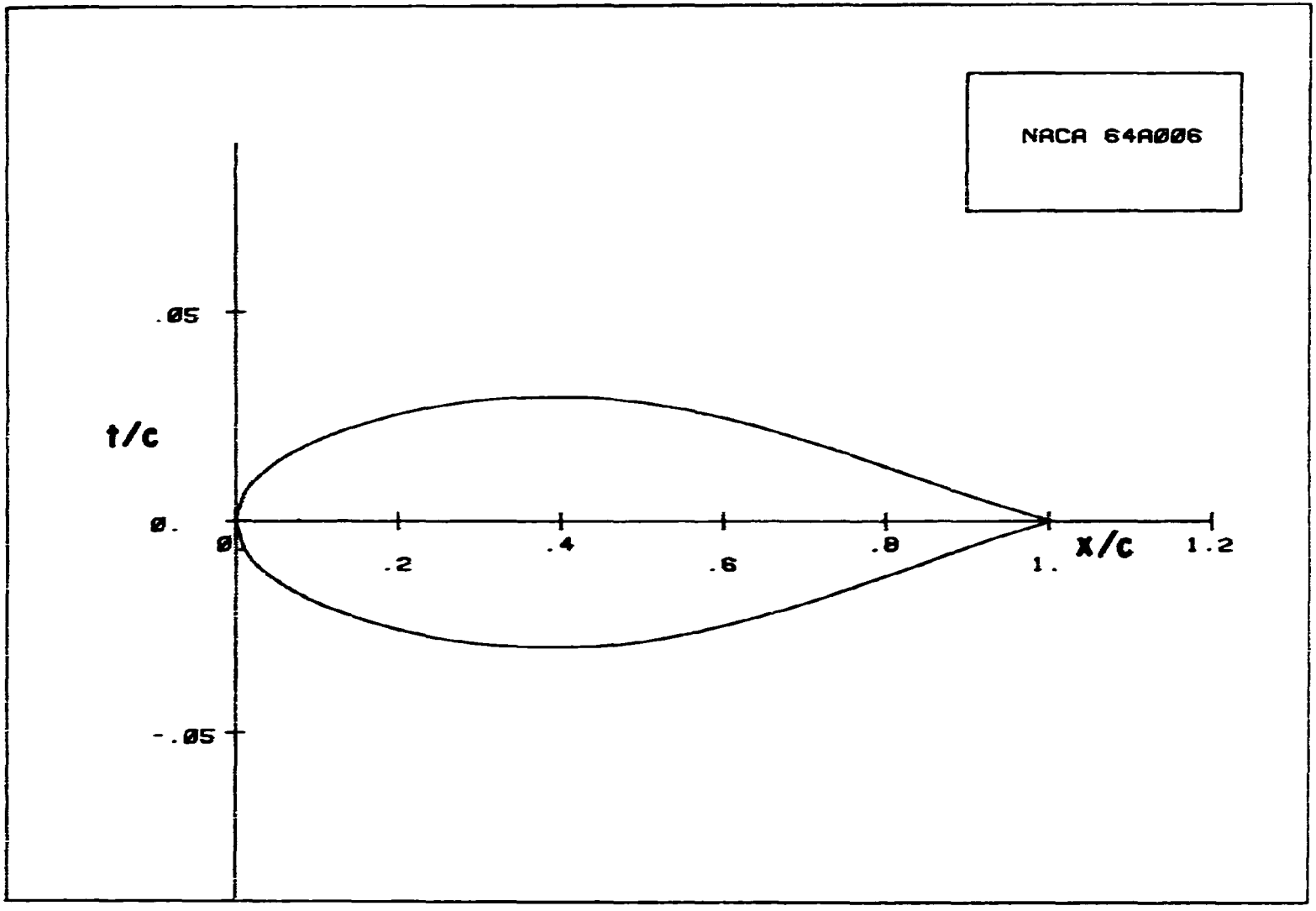

Figure 3. NACA 64A006 Airfoil Configuration

The steady-state solution was obtained by the SLOR method. A plot of the steady-state pressure curve is shown in Figure 4. In this figure it may be observed that there is a fairly strong shock on the airfoil between x/c = 0.64 and 0.69.

The governing differential equation of motion for this case is

$$\alpha'' + A_1\alpha' + A_2\alpha'' = A_3 c_m \tag{27}$$

where $A_3 = \pi/8\mu' k_c^2$ (see Equation 9).

To obtain the present response solution, it was first necessary to obtain a solution for the neutrally stable case. The moment coefficient $|c_{m\alpha}|$ and phase angle ψ (phase lag between c_m and α) were obtained by the time integration method by considering five cycles of forced motion. The pitching motion was sinusoidally forced with an amplitude of 0.5°. The values of $|c_{m\alpha}|$ and ψ obtained from this analysis were 0.8565 and -67.5 degrees, respectively. On the other hand the indicial method was employed in Reference 4 to obtain these results. The corresponding values of $|c_{m\alpha}|$ and ψ obtained in Reference 4 were 0.8617 and -68.87 degrees, respectively. The differences between the present results and those obtained in Reference 4 may be mainly due to the two different methods employed.

By assuming harmonic motion with frequency ω, i.e., $\alpha = \alpha_0 e^{i\omega t}$, and by relating the aerodynamic and structural constants, Equation 27 yields

$$A_1 = -A_3|c_{m\alpha}|\sin\psi \tag{28a}$$

$$A_2 = 1 + A_3|c_{m\alpha}|\cos\psi \tag{28b}$$

Assuming the value of A_3 equal to 1.333 (same as that used in Reference 4) and substituting the values described earlier for $|c_{m\alpha}|$ and ψ into Equations 28, A_1 and A_2 were obtained, respectively, as 1.05 and 1.437. These values correspond to the neutrally stable case. It is noted that in Reference 4, A_1 and A_2 were

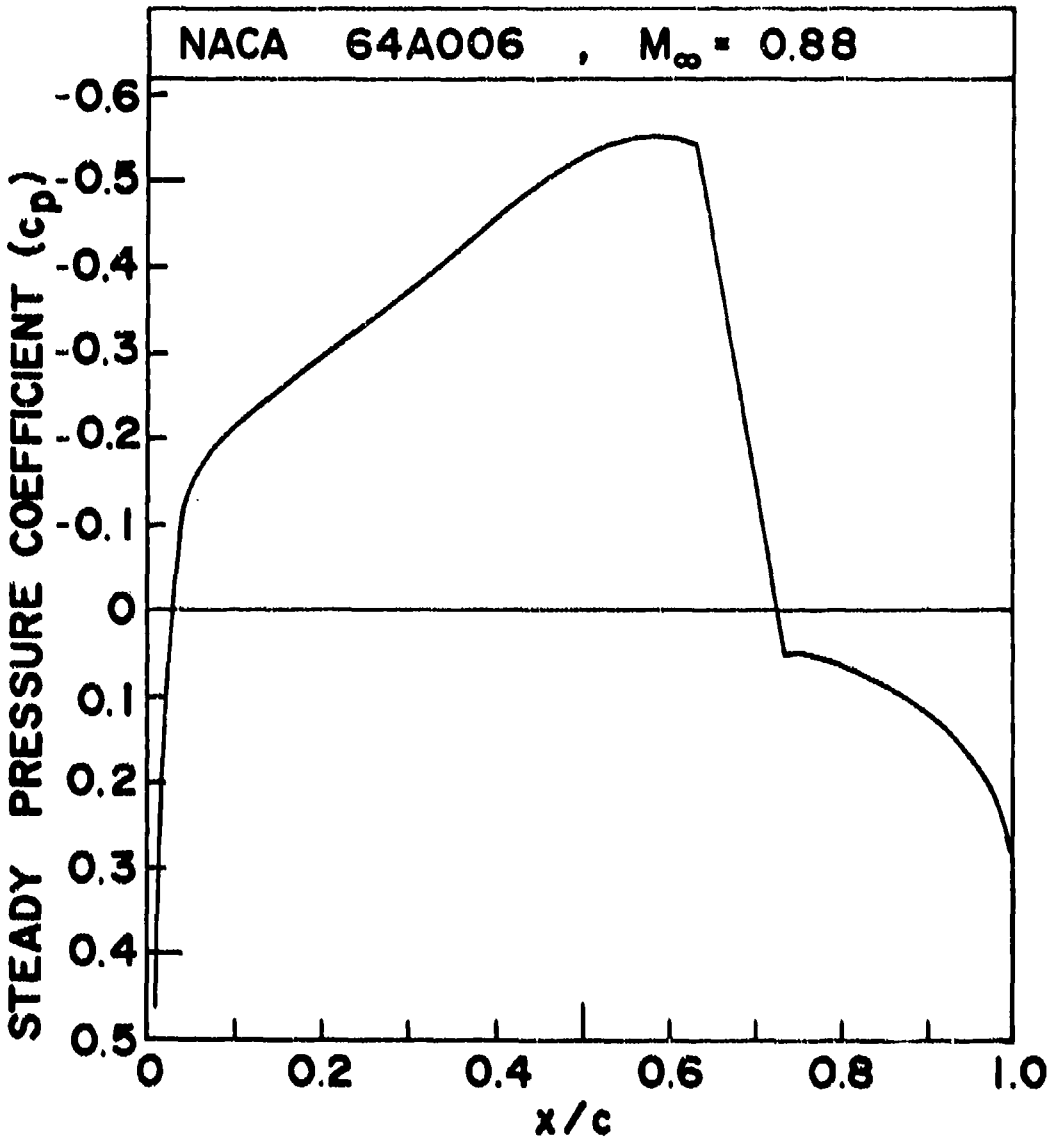

Figure 4. Distribution of Steady Pressure Coefficients for NACA 64A006 Airfoil at M = 0.88 by LTRAN2.

obtained as 1.072 and 1.414, respectively. The aeroelastic response analysis was then carried out by simultaneously integrating the aerodynamic and the airfoil motion equations. Different types of responses were obtained by parametrically varying the structural damping parameter A_1. The motion was forced for the first five cycles after which the pitching moment became periodic and the airfoil motion and aerodynamic response were left free to drive each other. The amplitude of the pitching angle was 0.5 degrees. The initial conditions for free motion were corresponding to $\alpha(0) = 0.0$, and $\alpha'(0) = 0.5$.

Response was obtained for values of the parameters corresponding to the neutrally stable case, i.e., $A_1 = 1.05$, $A_2 = 1.437$ and $A_3 = 1.333$. Figure 5 shows the response curves for the pitching angle α and the corresponding pitching moment c_m. In both curves, the first cycle is due to forced motion and the remaining cycles are due to free motion. Because the parameters corresponding to the flutter solution were chosen, the response in free motion is, as expected, very nearly periodic.

A diverging response was obtained when A_1 was assumed as 0.5. The results for the responses of both the pitching angle and the pitching moment are shown in Figure 6. A converging response was obtained when A_1 was assumed as 1.5 and the results are shown in Figure 7. These results are similar to those presented in Reference 4.

The above studies indicate that the general formulation of the problem is correct and the numerical integration procedure employed is quite accurate.

4.4.2 Flat Plate Pitching at $M_\infty = 0.70$

In the computer code LTRAN2, there is a capability to solve the linear form of Equation 2. This can be done by setting the input value for γ equal to -1.0. A response analysis for a flat plate pitching about mid-chord at Mach number $M = 0.7$ was performed for a reduced frequency $k_c = 0.1$. The present LTRAN2 (linear)

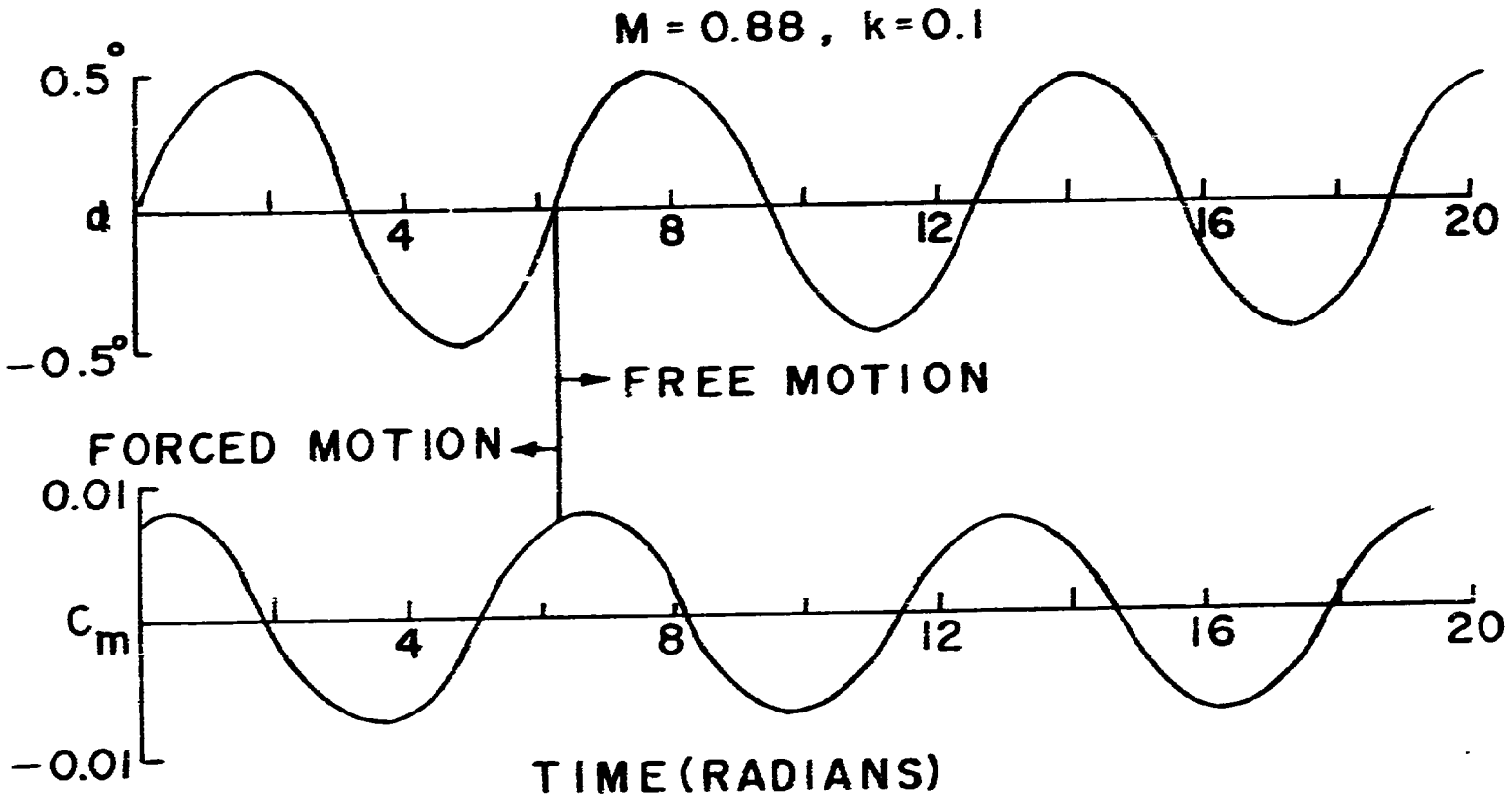

Figure 5. Pitching Motion Response for NACA 64A006 Airfoil Pitching about Mid-Chord (Neutrally Stable Case: $A_1 = 1.05$, $A_2 = 1.437$, $A_3 = 1.333$).

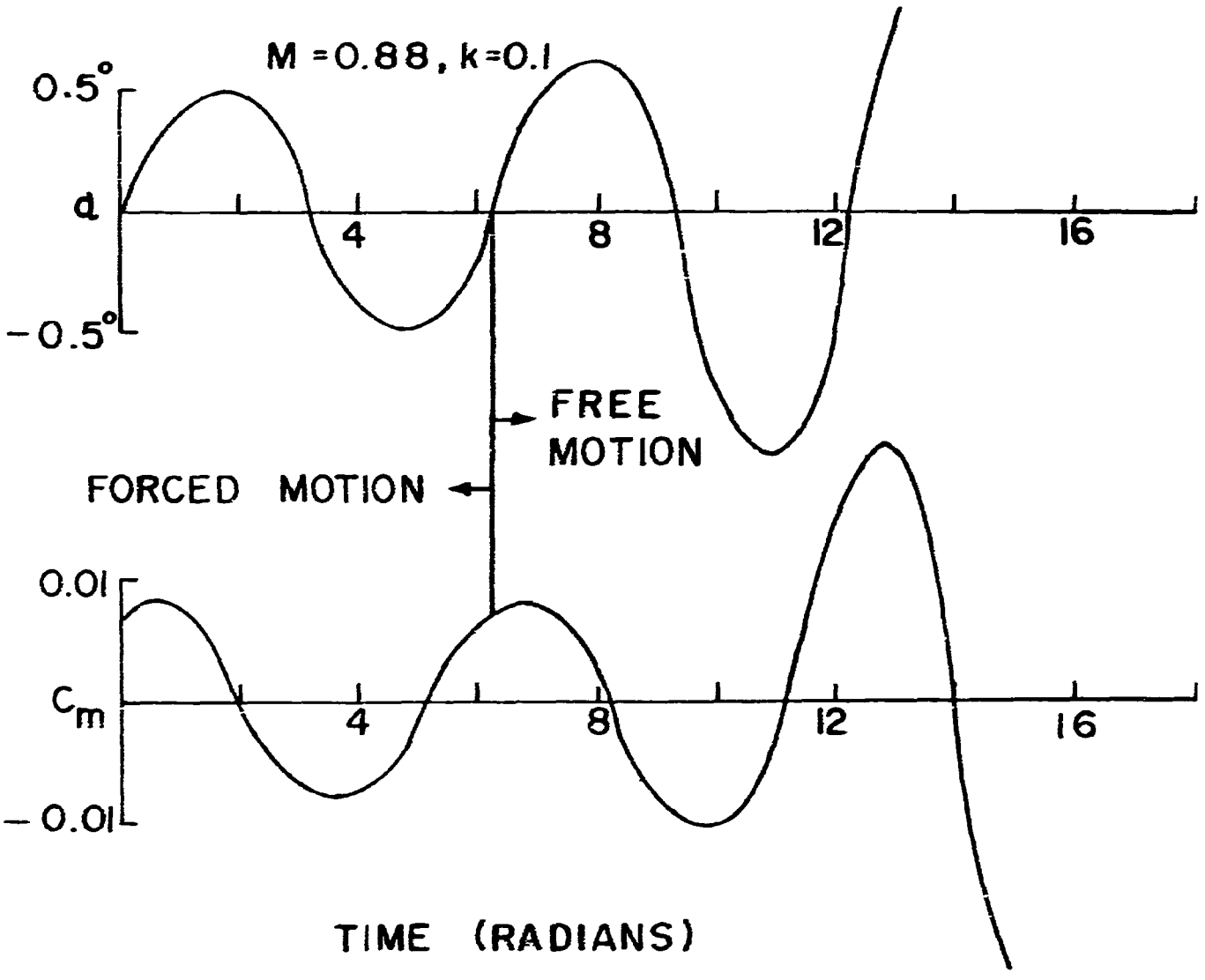

Figure 6. Pitching Motion Response for NACA 64A006 Airfoil Pitching about Mid-Chord (Diverging Case: $A_1 = 0.5$, $A_2 = 1.437$, $A_3 = 1.333$).

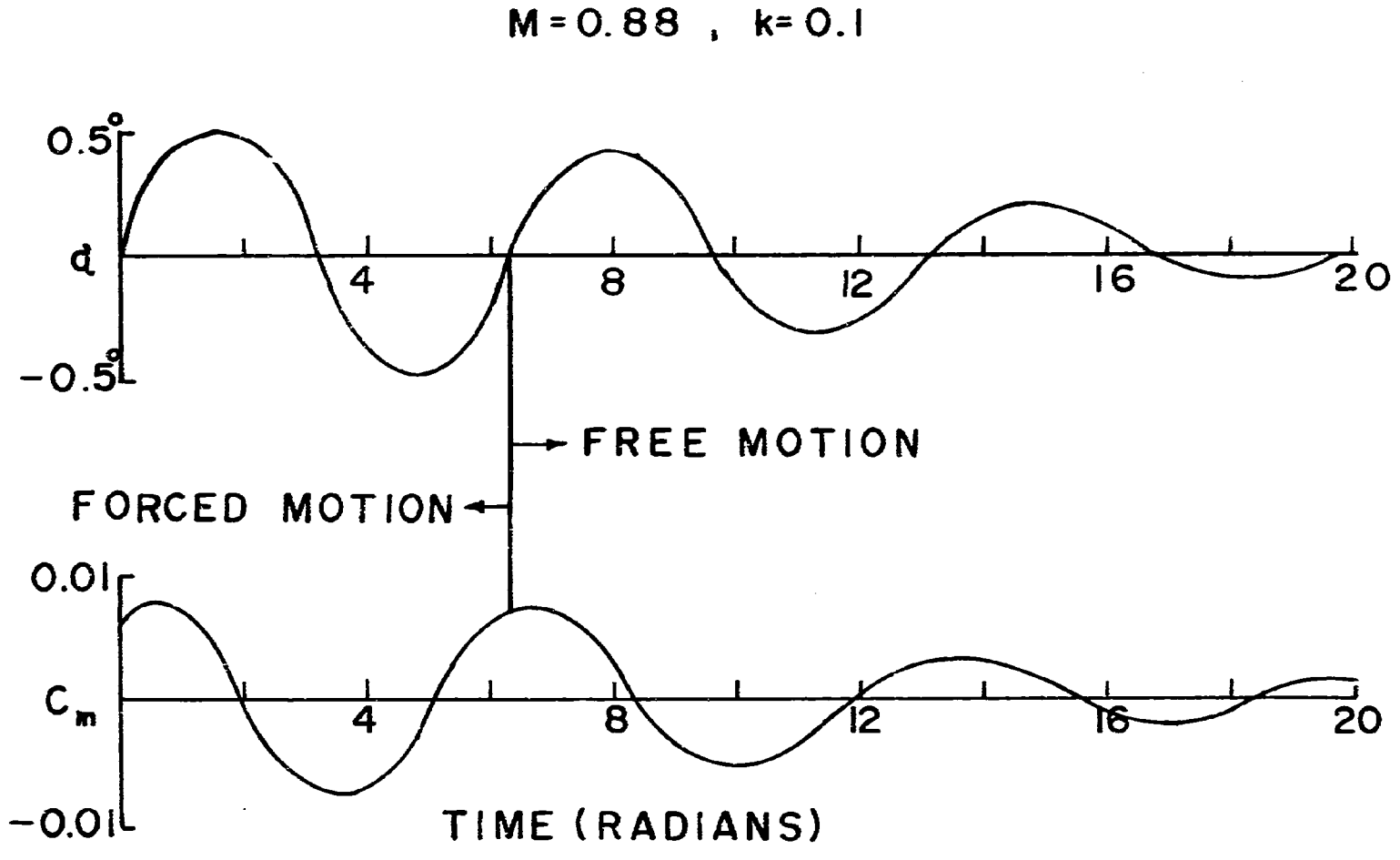

Figure 7. Pitching Motion Response for NACA 64A006 Airfoil Pitching about Mid-Chord (Converging Case: $A_1 = 1.5$, $A_2 = 1.437$, $A_3 = 1.333$).

results were compared with that obtained by quasi steady-state aerodynamic theory which is valid for reduced frequencies of the order $k_c = 0.1$.

The flat plate configuration was simulated in LTRAN2 by using data corresponding to a flat plate of a thickness-to-chord ratio of 0.01. In order to avoid numerical difficulty, the data for the airfoil configuration were started at $x/c = 0.003$ rather than at $x/c = 0.0$ (leading edge). The unsteady computations were started with zero steady-state pressure conditions.

Equation 9 as given in section II is the governing differential equation of motion for this case. The aerodynamic equation was integrated in time for four cycles by forcing a sinusoidal variation of pitching angle with amplitude of 0.01 radians. The free motion was started at the end of the fourth cycle. The initial conditions obtained for free motion were corresponding to $\alpha(0) = 0.0$ and $\alpha'(0) = 0.01$. The structural parameters for free motion were so selected that a converging type response could be obtained. The values for the damping parameter A_1, the stiffness parameter A_2 and the airfoil-air moment of inertia ratio μ' were 0.5, 1.5 and 1000, respectively. The value assumed for μ' was quite high when compared to the actual values for aircraft wings. However, this number was required in order to obtain a response solution that can be compared with quasi steady-state theory.

The converging type response curves obtained for pitching angle α and pitching moment c_m are shown in Figure 8. In the same figure the responses obtained by employing the quasi steady-state aerodynamic theory are also shown. These responses were obtained by solving the differential Equation 11 for the same values of A_1, A_2, μ', $\alpha(0)$ and $\alpha'(0)$ as used for LTRAN2. The two sets of solutions are, in general, in fairly good agreement.

Small differences in amplitude and phase angle in Figure 8 between the two sets of results are mainly due to the difference between the two methods. It may

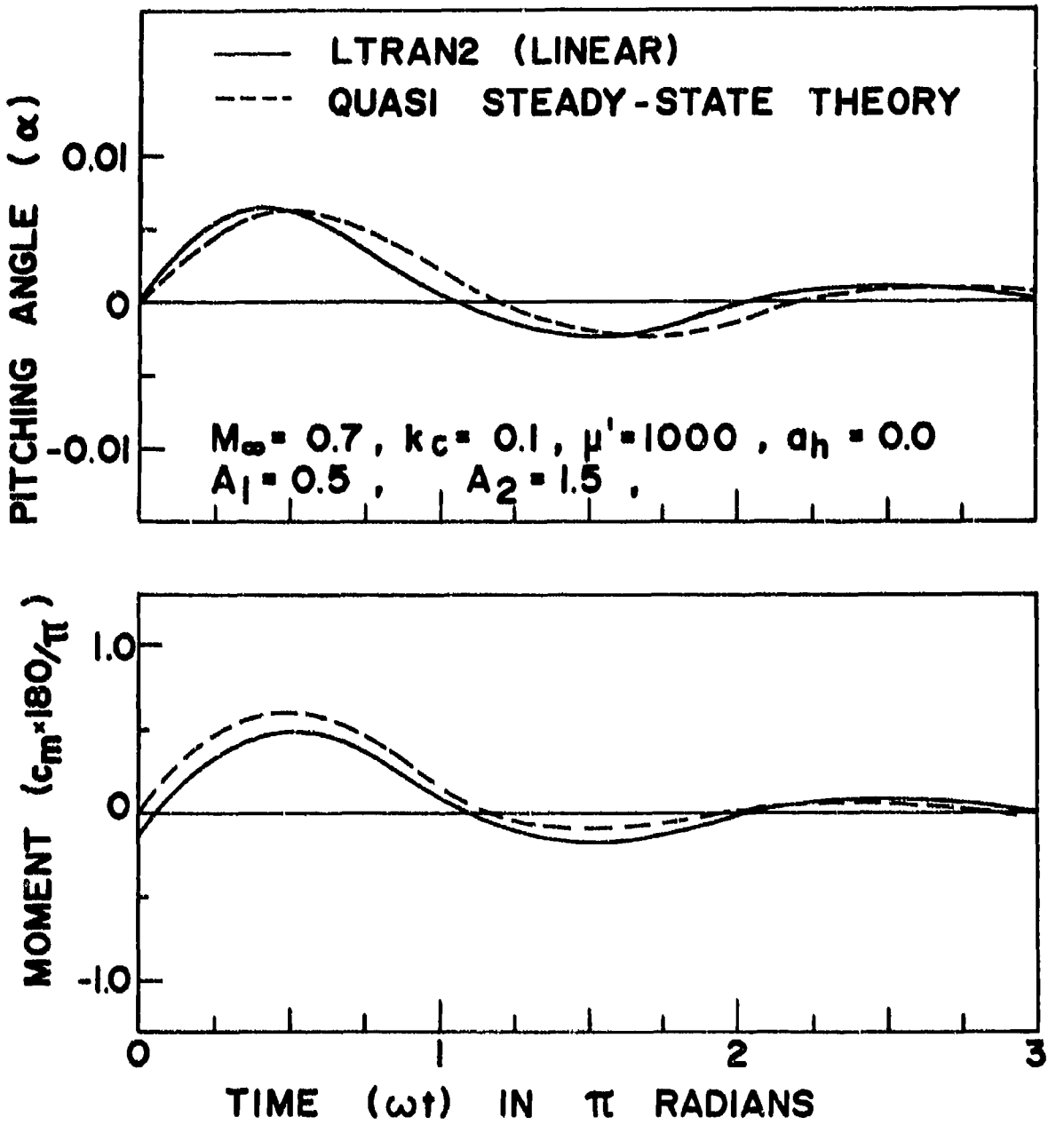

Figure 8. Comparison of the Pitching Responses Obtained by LTRAN2 and Quasi Steady-State Theory for a Flat Plate Pitching about Mid-Chord.

be observed that there is no phase lag between the pitching angle and the corresponding moment in the quasi steady-state solution but there is some phase lag in the LTRAN2 solution. Therefore, the effective aerodynamic dampings in the system between the two methods are different which may cause the discrepancy between the two sets of curves. Such discrepancy becomes larger for smaller values of μ' since aerodynamic damping is inversely proportional to μ'.

At this point, it may be noted that LTRAN2 is based on the low frequency approximation which is more valid for Mach numbers near unity. The discrepancy found in the two sets of curves may also be partly due to the low value of Mach number (0.7) considered.

4.4.3 Flat Plate Plunging at M = 0.7

In this case, response results were obtained for a flat plate with only a single plunging degree of freedom. The Mach number and reduced frequency k_c considered were equal to 0.7 and 0.1, respectively. Flat plate conditions were simulated in the same manner as discussed earlier. Results were obtained both from LTRAN2 (linear) and quasi steady-state theory.

The governing differential equation of motion for this case is given in Section II as Equation 15. The aerodynamic equation was first integrated by LTRAN2 for four cycles by forcing a sinusoidal plunging motion with amplitude of plunging displacement $\delta = h/c = 0.1$. This corresponds to an amplitude of 0.01 radians for the induced angle of attack $\alpha_1 = k_c\delta'$.

The free motion was started with initial conditions corresponding to $\alpha_1(0) = 0.0$ ($\delta = 0.1$) and $\alpha_1'(0) = 0.01$ ($\delta' = 0.0$). The structural parameters were selected so that a converging type response could be obtained. The values assumed for the structural damping parameter B_1, the structural stiffness parameter B_2 and the airfoil-air mass ratio μ were equal to 0.0, 1.0, and 100, respectively. Response curves obtained from LTRAN2 for plunging displacement δ

and lifting force coefficient c_ℓ are shown in Figure 9. In the same figure the corresponding results obtained by quasi steady-state theory are also shown. These results were obtained by solving the differential equation 17 based on the same initial conditions and structural parameters as used in LTRAN2.

Response results obtained by both methods compare fairly well. The small differences in phase angles and amplitudes may be mainly due to the difference in the methods.

4.5 Two Degree of Freedom Systems (Pitching and Plunging)

In the response studies of the two degree of freedom systems, two cases were analyzed. One case is a flat plate pitching about the mid-chord at $M_\infty = 0.7$ and the other is a NACA 64A006 airfoil pitching about the quarter chord at $M_\infty = 0.85$. Response results were obtained by parametrically varying the airfoil-air mass ratio μ. In all the examples, the values of reduced frequency k_c and radius of gyration r_α were assumed as 0.1 and 0.5, respectively. The mechanical damping was assumed as zero ($\zeta_h = \zeta_\alpha = 0$).

4.5.1 Flat Plate Plunging and Pitching about Mid-Chord at M = 0.7

In this case response studies were performed for a flat plate pitching about mid-chord at a subsonic Mach number $M_\infty = 0.7$. Both the LTRAN2 (linear) code and the Kernel Function method were used so that the two sets of results can be compared.

Before starting the response analysis it was necessary to find the aeroelastic parameters corresponding to a neutrally stable condition. Equations 20 discussed in Section II are the governing equations of motion for this case. The aeroelastic parameters include: flight speed parameter U^*, airfoil-air mass ratio μ, position of the mass center x_α, plunge to pitch frequency ratio ω_h/ω_α, radius of gyration r_α, damping parameters ζ_h and ζ_α, and position of elastic axis a_h. The values for x_α, ω_h/ω_α, r_α, ζ_h, ζ_α, and a_h were assumed as 0.0, 0.2, 0.5,

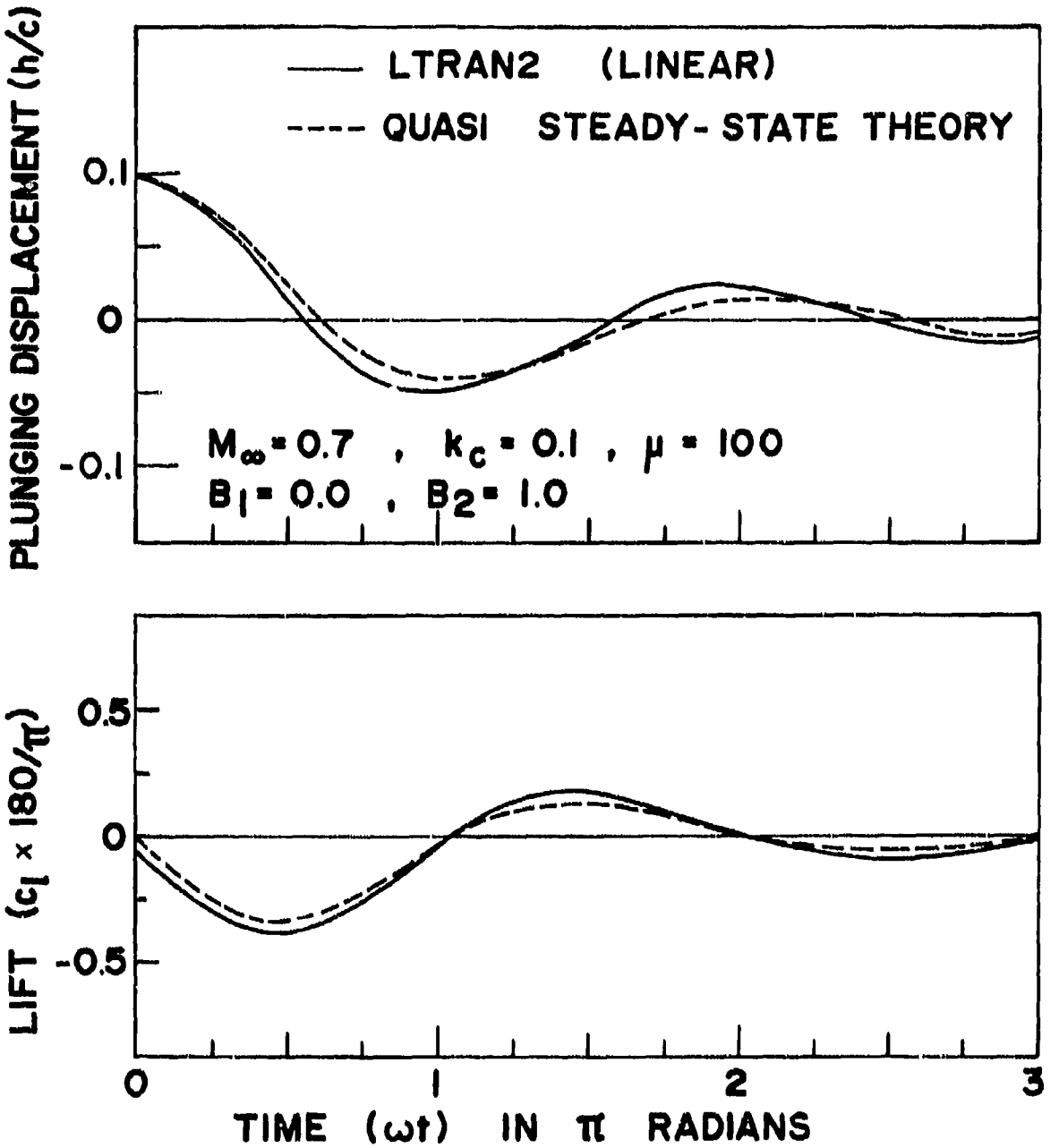

Figure 9. Comparison of the Plunging Responses Obtained by LTRAN2 and Quasi Steady-State Theory for a Flat Plate.

0.0, 0.0 and 0.0, respectively.

In order to obtain the values of k_c, U^* and μ corresponding to the neutrally stable condition, the U-g method was used. A detailed discussion of this method is given in Reference 2.

To use the U-g method, it is necessary to obtain a table of aerodynamic coefficients similar to those obtained in Reference 2. Table 1 shows the aerodynamic coefficients of c_{ℓ_δ}, c_{ℓ_α}, c_{m_δ} and c_{m_α} obtained by using the time integration method of LTRAN2 (linear) and Kernel Function method for various values of reduced frequency k_c. Agreement is good between the two methods.

A flutter analysis was carried out for various values of airfoil-air mass ratio μ by the U-g method. Figure 10 shows the curves for flutter speed and corresponding reduced frequency versus the airfoil-air mass ratio μ obtained by both methods. Excellent agreement is observed.

Any point on the curves shown in Figure 10 represents a neutrally stable state whereas the zones below and above the curves represent stable and unstable conditions, respectively. Response analyses were carried out for stable, neutrally stable and unstable conditions by selecting the aeroelastic parameters based on any selected point in the flutter speed curves. Because the time integration method was used in performing the response studies, it was essential that the flutter curves be obtained by using the time integration method instead of the indicial and relaxation methods as used in Reference 2.

The governing equations of motion for this case are given by Equation 20 of Section II. To begin with, the aerodynamic equation was integrated in time for four cycles by forcing a sinusoidal pitching motion with amplitude of 0.01 radians. In the fourth cycle the aerodynamic force responses became almost periodic. After that, the free motion was started by simultaneously integrating the structural and aerodynamic equations. This was started with initial conditions with $\xi(0) = 0$, $\xi'(0) = 0$, $\alpha(0) = 0$, and $\alpha'(0) = 0.01$.

Table 1

AERODYNAMIC COEFFICIENTS FOR FLAT PLATE

PITCHING ABOUT MID-CHORD AT M = 0.7

Aerodynamic Coeff.	Method	Reduced Frequency $k_c = \omega c/U$					
		0.05		0.10		0.15	
		Real	Imag.	Real	Imag.	Real	Imag.
c_{ℓ_δ}	1	0.0669	0.4225	0.1700	0.8000	0.3038	1.134
	2	0.0616	0.3974	0.1666	0.7190	0.2719	0.9876
c_{ℓ_α}	1	8.449	-1.338	8.001	-1.701	7.557	-2.025
	2	7.964	-1.133	7.240	-1.488	6.671	-1.570
c_{m_δ}	1	0.0151	0.0952	0.0479	0.1787	0.0954	0.2486
	2	0.0174	0.0990	0.0501	0.1780	0.0865	0.2425
c_{m_α}	1	1.904	- .3016	1.787	- .4788	1.657	- .6361
	2	1.985	- .3500	1.794	- .5117	1.640	- .5996

Method 1: Time Integration by LTRAN2 (linear).
Method 2: Kernel Function Method.

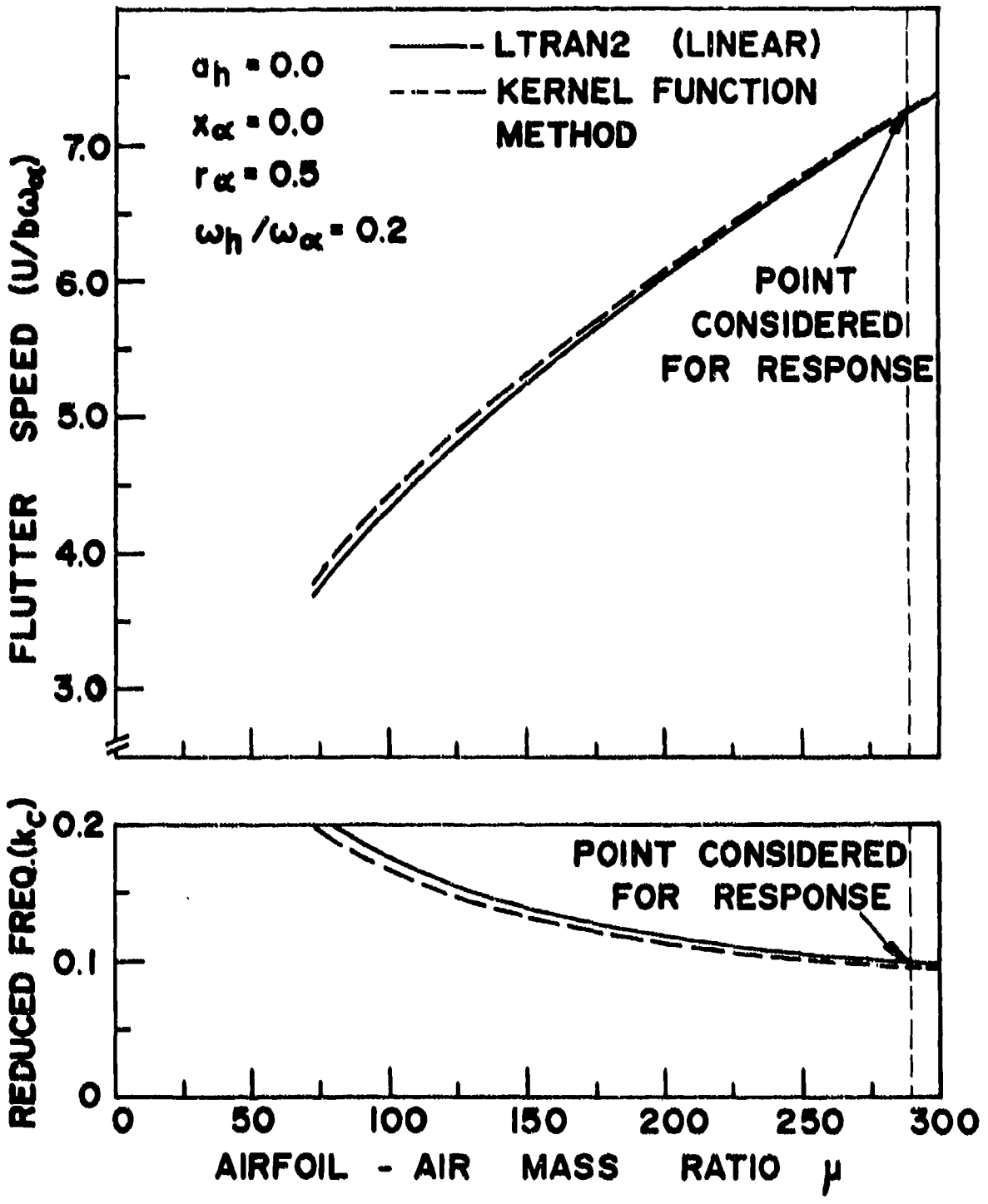

Figure 10. Effect of Airfoil-Air Mass Ratio on Flutter Speed for Flat Plate at M = 0.7

Aeroelastic parameters for the neutrally stable condition were selected from a point on the flutter speed curves in Figure 10 at $k_c = 0.1$. The corresponding values of μ and U^* were equal to 289.5 and 7.23, respectively. These values were substituted into Equation 20 and the response analysis was carried out. Response curves for pitching angle α and the corresponding pitching moment c_m for about six cycles are shown in Figure 11. After small initial disturbances (due to initial conditions) both response curves show a perfect periodic behavior. Similar curves obtained for plunging displacement ξ and corresponding lifting force c_ℓ are shown in Figure 12. These curves also show a perfect periodic behavior after some small initial disturbances. It is seen that the neutrally stable conditions obtained by the present response method are in good agreement with those obtained by the U-g method based on both the time integration and the Kernel Function method.

In Figure 11, the response curves for pitching displacement α and pitching moment c_m for the stable and unstable conditions are also shown. These were obtained by changing the airfoil-air mass ratio μ. For unstable response the μ value assumed was 10% lower than that corresponding to the neutrally stable condition. This point is in the unstable zone of Figure 10. On the other hand, for stable response the μ value selected was 10% higher than that corresponding to the neutrally stable condition. The corresponding stable and unstable responses for plunging displacement ξ and lifting force c_ℓ are also shown in Figure 12. It is seen that the stable and unstable conditions obtained by the U-g method produced converging and diverging responses, respectively.

It was also of interest to study the effect of airfoil-air mass ratio (altitude) μ on the peak amplitudes of the response curves. In this analysis, the peak amplitudes corresponding to the second free cycle were considered. Figure 13 shows plots of the ratio of the second cycle peak amplitude to the amplitude of the neutrally stable curve versus the ratio of airfoil-air mass

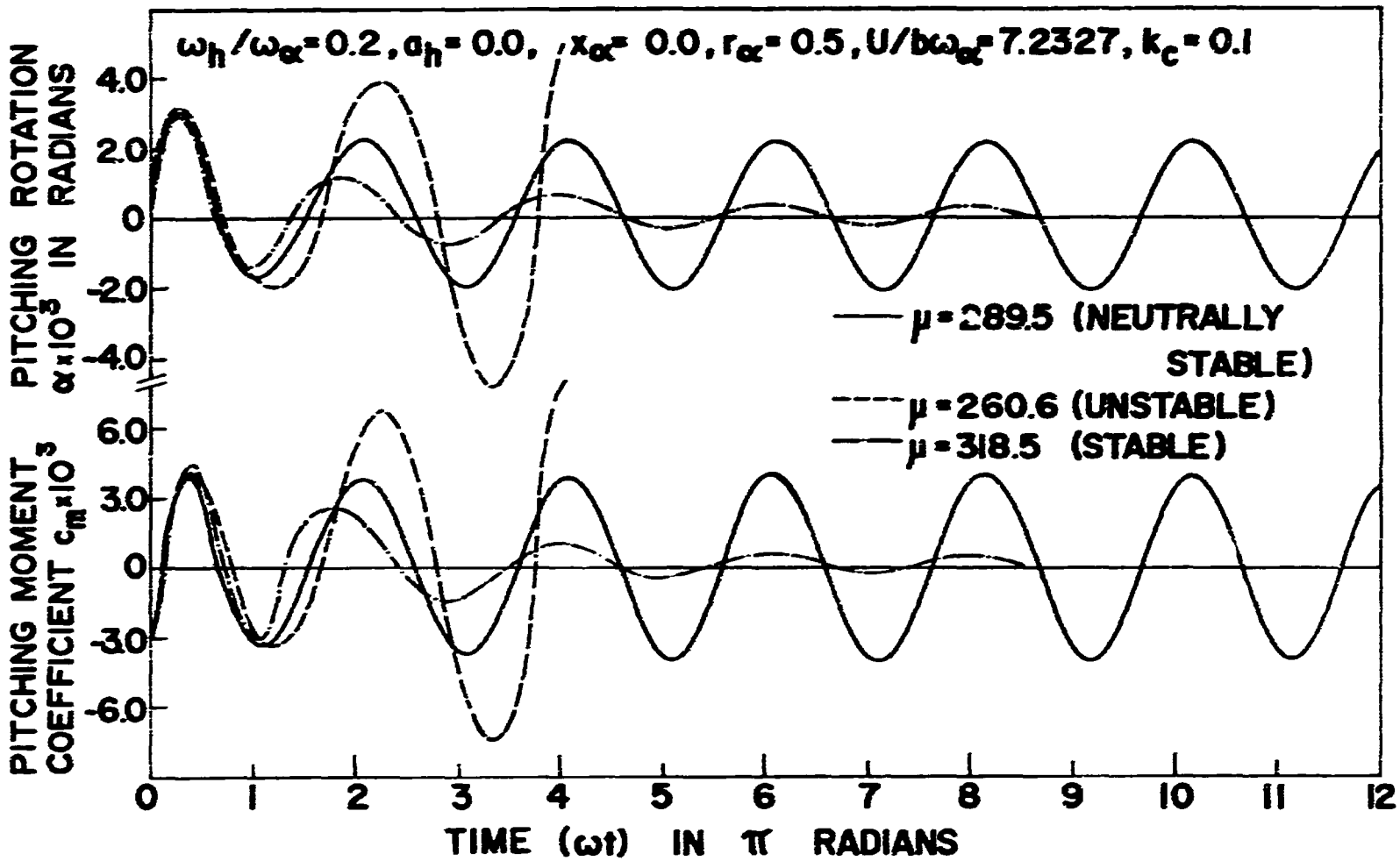

Figure 11. Effect of Airfoil-Air Mass Ratio (Altitude) on Pitching Rotation (α) and Pitching Moment (c_m) for Flat Plate at M = 0.7.

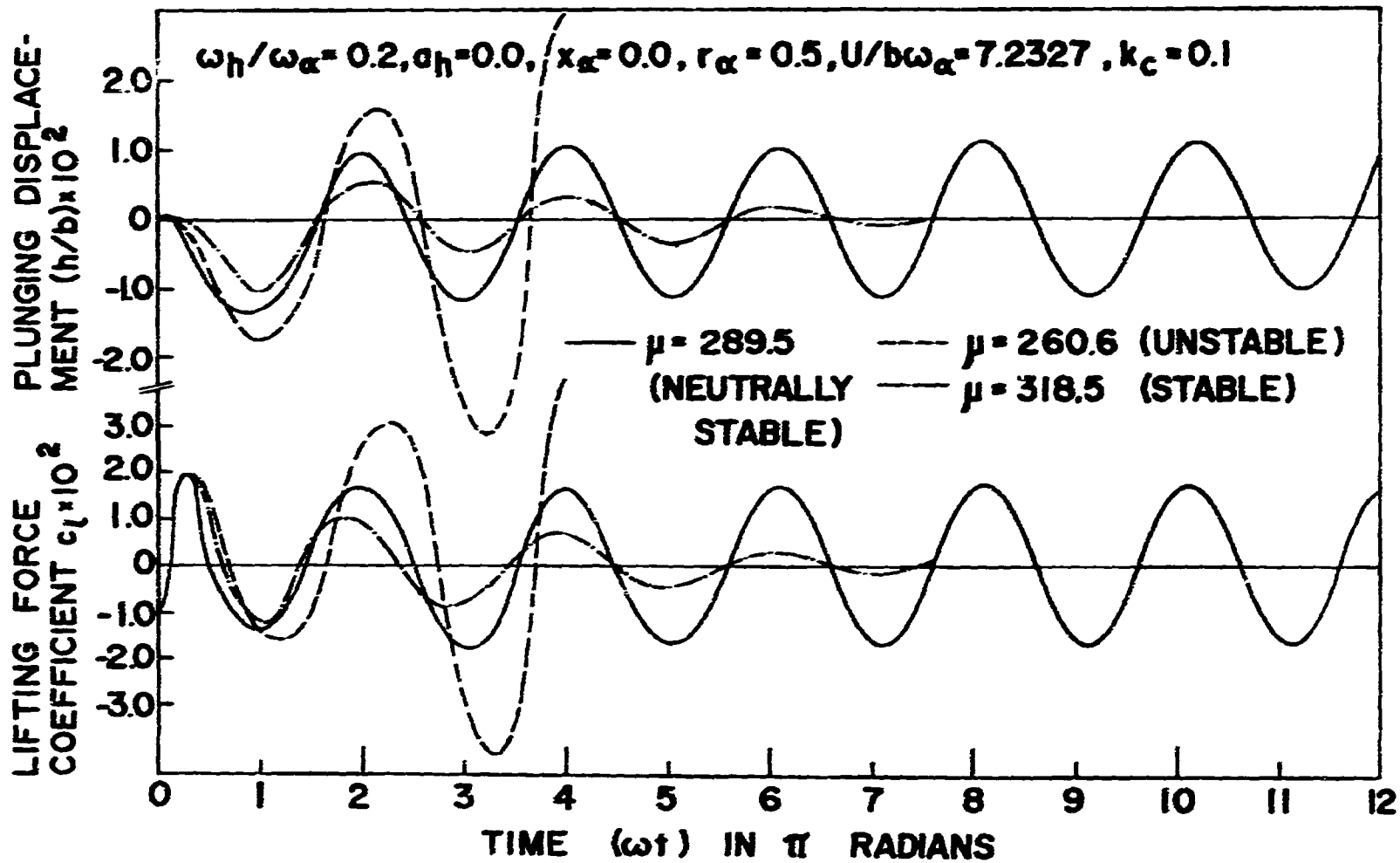

Figure 12. Effect of Airfoil-Air Mass Ratio (Altitude) on Plunging Displacement (ξ) and Lifting Force Coefficient (c_ℓ) for Flat Plate at M = 0.7.

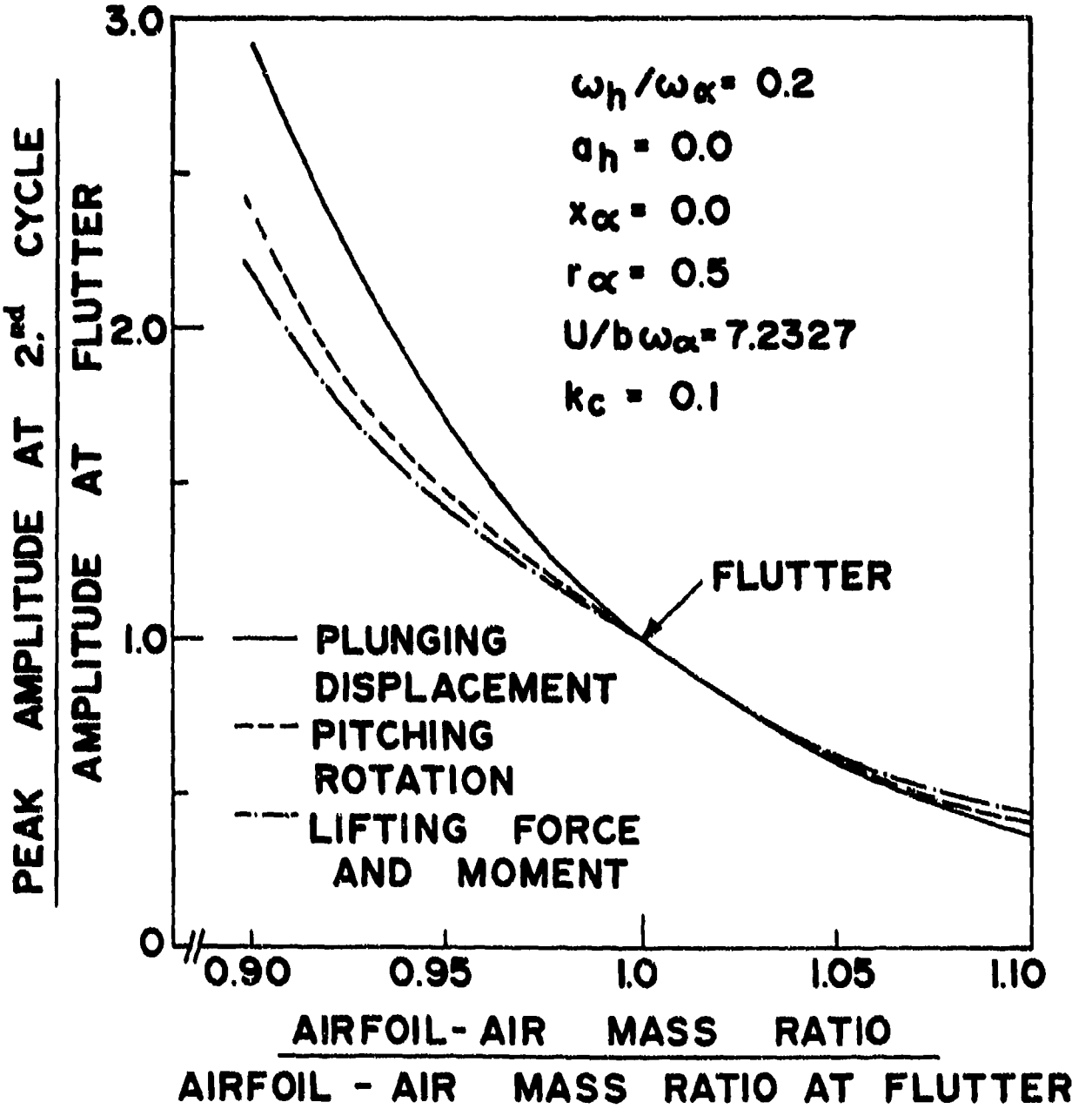

Figure 13. Effect of Airfoil-Air Mass Ratio on Peak Amplitudes of Responses for Flat Plate at M = 0.7.

ratio μ to the airfoil-air mass ratio at the neutrally stable condition. The plots include four curves for plunging displacement, lifting force, pitching displacement and pitching moment, respectively.

From Figure 13 it may be observed that the curve corresponding to plunging displacement is steeper than the other three curves. All the curves assume a similar trend below the neutrally stable point. The curves for lifting force and moment are very close to each other and they virtually coincide. Such curves may be used to study the aeroelastic behavior of the system near the neutrally stable point.

4.5.2 NACA 64A006 Airfoil Plunging and Pitching about Quarter Chord at M = 0.85

In the flutter analysis performed in References 6 and 7, a "transonic dip" phenomenon was observed for the NACA 64A006 airfoil. Flutter speeds reached a minimum in the neighborhood of M = 0.85. From the aeroelastic point of view, this Mach number is the critical value. Hence, in this study aeroelastic response analysis was carried out at M = 0.85.

In this case a NACA 64A006 airfoil pitching about the quarter chord (a_h=-.5) at M = 0.85 was considered. The procedure for obtaining the responses is the same as that described for the case of the flat plate.

The steady-state pressure distribution curve obtained from LTRAN2 (nonlinear) is shown in Figure 14. In the same figure pressure curves obtained by STRANS2 (Reference 2) and by experimental method (Reference 13) are also shown for comparison. In general, all three curves agree fairly well.

Using the steady-state initial conditions, unsteady computations were carried out by using LTRAN2 (nonlinear). The time integration method was employed to obtain the aerodynamic coefficients c_{ℓ_δ}, c_{ℓ_α}, c_{m_δ} and c_{m_α}. The coefficients for various values of reduced frequency k_c are shown in Table 2. In the same table, the aerodynamic coefficients computed by UTRANS2 and the indicial method in Reference 2 are also given. In general, all three methods agree well. It may be noted that

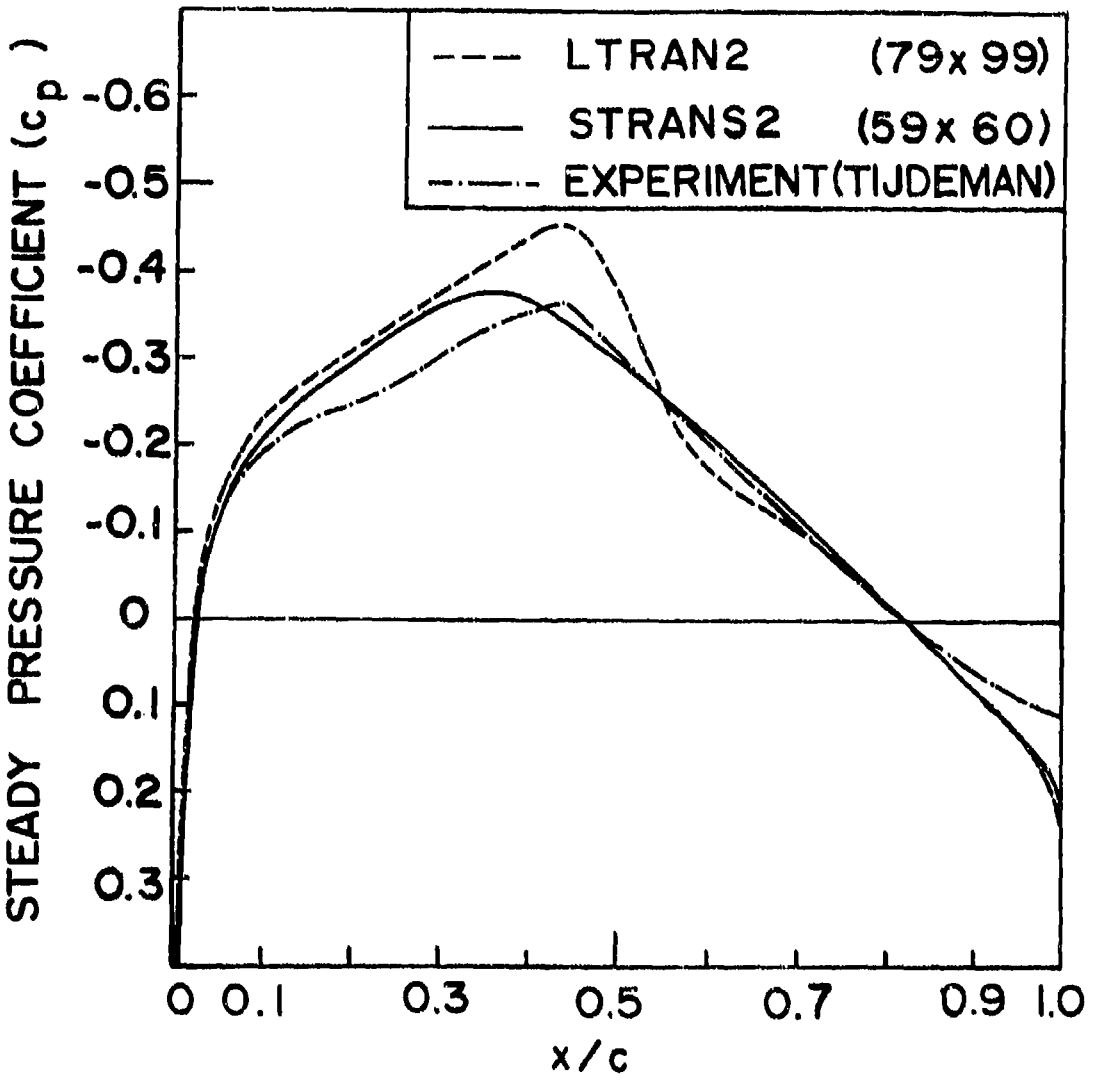

Figure 14. Distribution of Steady Pressure Coefficients for NACA 64A006 Airfoil at M = 0.85.

the results obtained by the time integration method are expected to be more accurate than those obtained by the other two methods for $k_c < 0.2$.

Based on the coefficients given in Table 2, flutter analysis was carried out by the U-g method. Plots of flutter speed and corresponding reduced frequency versus airfoil-air mass ratio are shown in Figure 15. The values assumed for the aeroelastic parameters were: position of elastic axis $a_h = -0.5$; position of mass center $x_\alpha = 0.25$; plunge to pitch frequency ratio $\omega_h/\omega_\alpha = 0.2$; radius of gyration $r_\alpha = 0.5$; and damping parameters $\zeta_h = 0$ and $\zeta_\alpha = 0$.

The results obtained from the relaxation method (UTRANS2) and the indicial method are, in general, in good agreement. The curves obtained from the time integration method, however, differ from the other two sets of curves to some extent. Such discrepancy may be due to the differences in the methods and the numerical errors in computations. It may be noted here that both the relaxation and indicial methods are based on time-linearized equations in the unsteady aerodynamic computations and the provision of treating the shock wave motion is lacking. The time integration method has no such time-linearization assumption and it can efficiently treat shock movement. Thus the presence of shock for the Mach number considered might have also caused the discrepancy in these flutter results.

In the response analysis, Equation 20 is the governing aeroelastic equation of the system. Reduced frequency was assumed as $k_c = 0.1$. To start with, the aerodynamic equation was integrated in time for six cycles by forcing a sinusoidal pitching motion with amplitude of 0.01 radians. In the sixth cycle the forced responses in LTRAN2 became almost periodic. From this point onwards free motion was considered by simultaneously integrating the aerodynamic and structural equations. Free motion was started with initial conditions with $\xi(0) = 0$, $\xi'(0) = 0$, $\alpha(0) = 0$, and $\alpha'(0) = 0.01$.

Table 2

AERODYNAMIC COEFFICIENTS FOR NACA 64A006

PITCHING ABOUT THE QUARTER CHORD AXIS AT M = 0.85

Aerodynamic Coeff.	Method	Reduced Frequency $k_c = \omega c/U$					
		0.05		0.10		0.15	
		Real	Imag	Real	Imag	Real	Imag
c_{ℓ_δ}	1	0.302	0.678	0.616	1.067	0.867	1.335
	2	0.136	0.666	0.492	1.180	0.938	1.470
	3	0.163	0.626	0.480	0.962	0.783	1.148
c_{ℓ_α}	1	13.561	-6.038	10.669	-6.160	8.900	-5.780
	2	13.310	-2.720	11.820	-4.920	9.770	-6.250
	3	11.803	-3.701	9.160	-4.491	7.223	-4.076
c_{m_δ}	1	0.010	- .038	0.011	- .068	- .028	- .104
	2	- .001	- .034	- .005	- .068	- .012	- .102
	3	0.004	- .026	0.009	- .054	0.013	- .089
c_{m_α}	1	- .749	- .201	- .675	- .107	- .691	+ .185
	2	- .676	0.021	- .677	0.053	- .677	0.082
	3	- .501	- .071	- .510	- .147	- .514	- .210

Method 1. LTRAN2 Time Integration (79 x 99)
Method 2. LTRAN2 Indicial Method (79 x 99)
Method 3. STRANS2 and UTRANS2 Relaxation method (59 x 60)

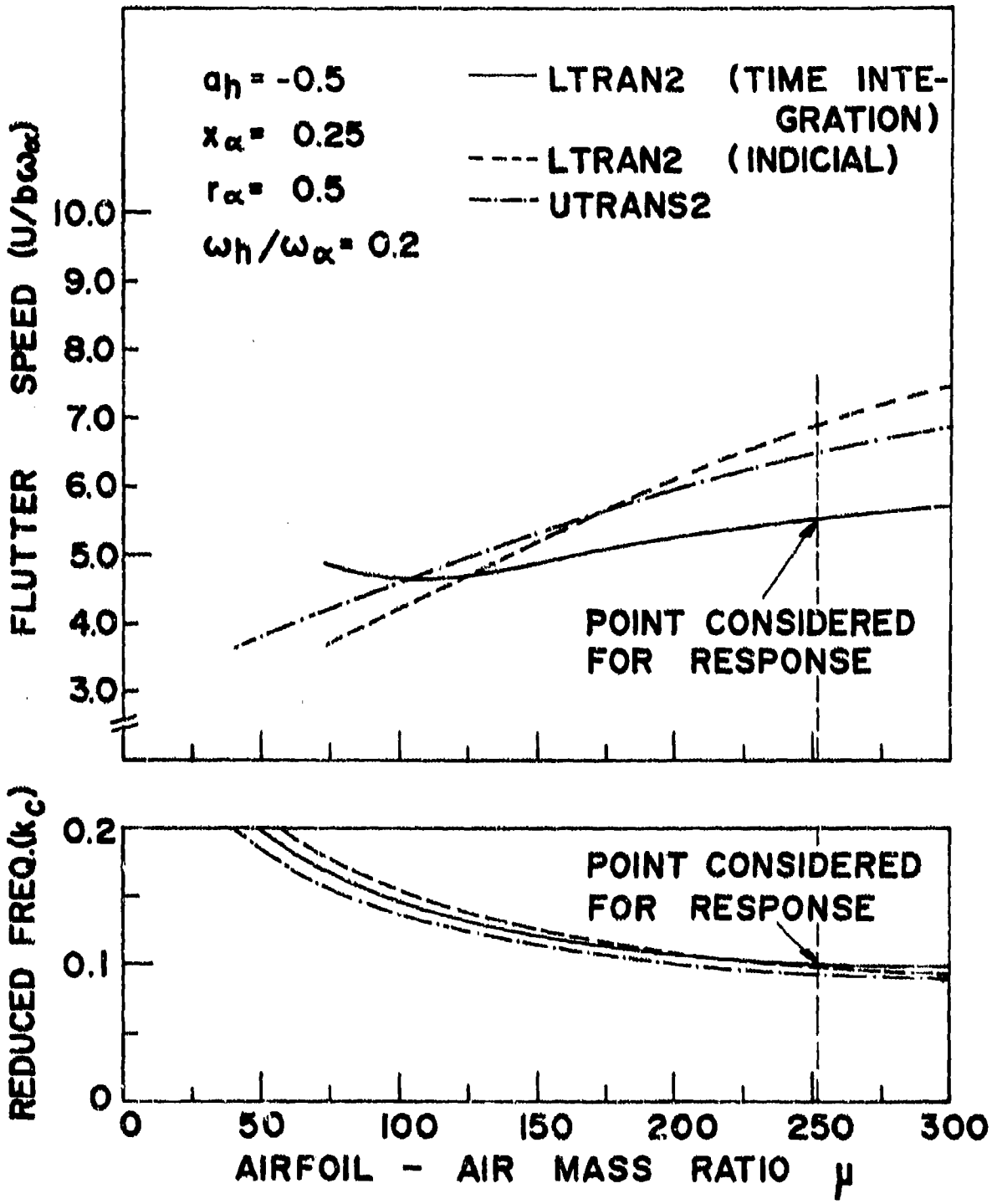

Figure 15. Effect of Airfoil-Air Mass Ratio on Flutter Speed for NACA 64A006 Airfoil at M = 0.85.

Stable, neutrally stable, and unstable responses were obtained by parametrically varying the airfoil-air mass ratio μ. A neutrally stable response was obtained by considering a point on the flutter speed curve obtained by the time integration method in Figure 15 at $k_c = 0.1$. The corresponding values of μ and U^* thus obtained were equal to 252.5 and 5.5, respectively. These values along with the other aeroelastic parameters ($a_h = -.5$, $x_\alpha = 0.25$, $\omega_h/\omega_\alpha = 0.2$, $r_\alpha = 0.5$, $k_c = 0.1$) were substituted into Equation 20 and the response analysis was carried out. The responses for plunging displacement and corresponding lifting force obtained from LTRAN2 are shown in Figure 16. After some small initial disturbances due to the initial conditions, the response curves show ideal periodic behavior.

The corresponding stable response curves for pitching displacement α and pitching moment c_m are shown in Figure 17. These curves are shown only from the second cycle of the free motion. As compared to Figure 16, there were quite pronounced initial disturbances due to initial conditions in the first cycle. However, the responses became almost periodic after the third cycle of free motion.

One possible reason for the pronounced initial disturbances in the first cycle of the free pitching response is that the pitching axis is located at the quarter chord. The moment values at the quarter chord are very small and the plunging motion initially dominates the response. Hence, the pitching responses require more cycles to become periodic when compared to the plunging responses. It may be noted that for the case of flat plate pitching about the mid-chord, the order of initial disturbances was the same for both plunging and pitching responses (See Figures 11 and 12). This may be due to the fact that the moment value about the mid-chord is larger than that about the quarter chord.

The curves for neutrally stable responses presented in Figures 16 and 17 show that the neutrally stable conditions obtained by the present response method are in good agreement with those obtained by the U-g method based on the time integration

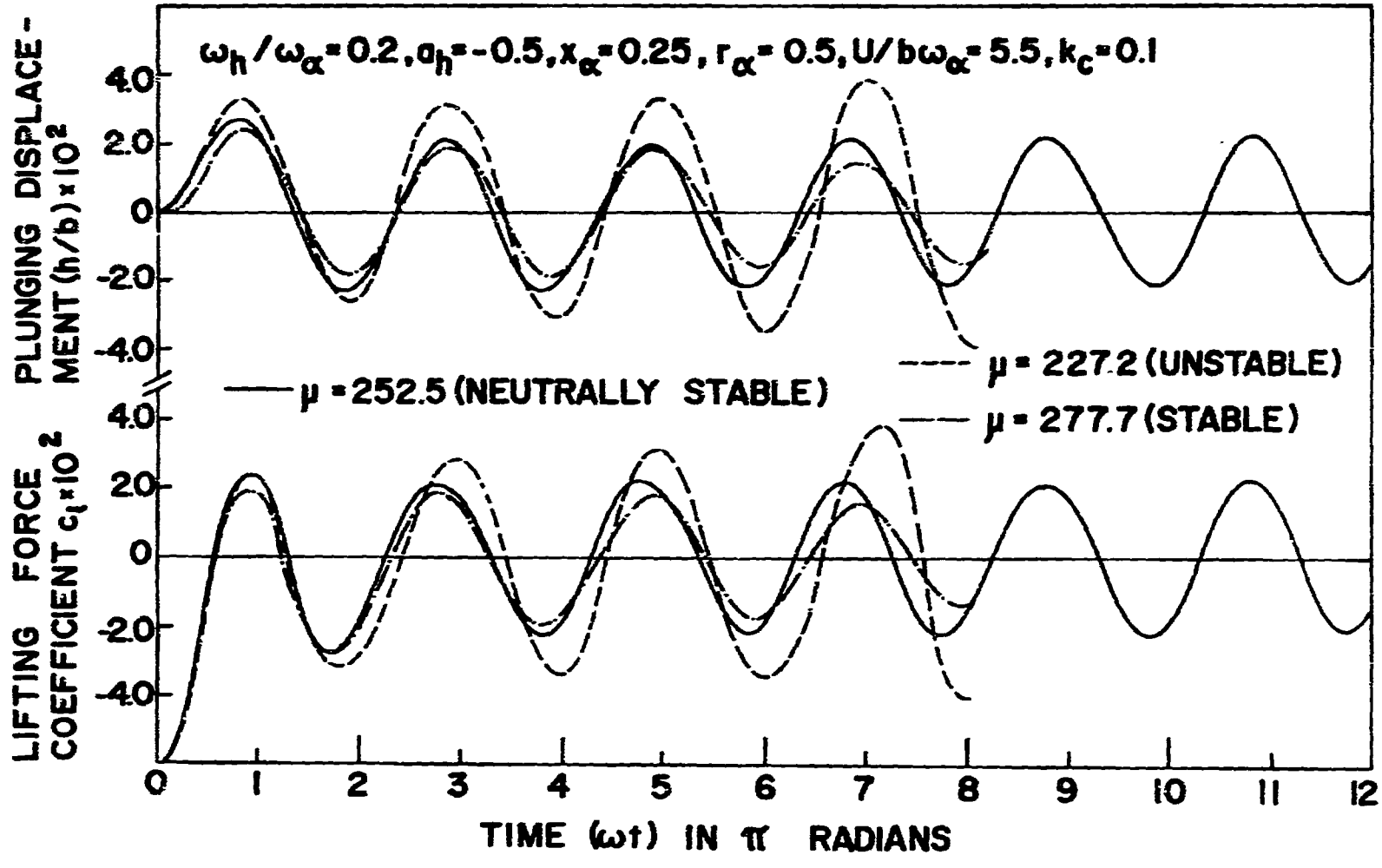

Figure 16. Effect of Airfoil-Air Mass Ratio (Altitude) on Plunging Displacement (ξ) and Lifting Force Coefficient (c_l) for NACA 64A006 Airfoil at M = 0.85.

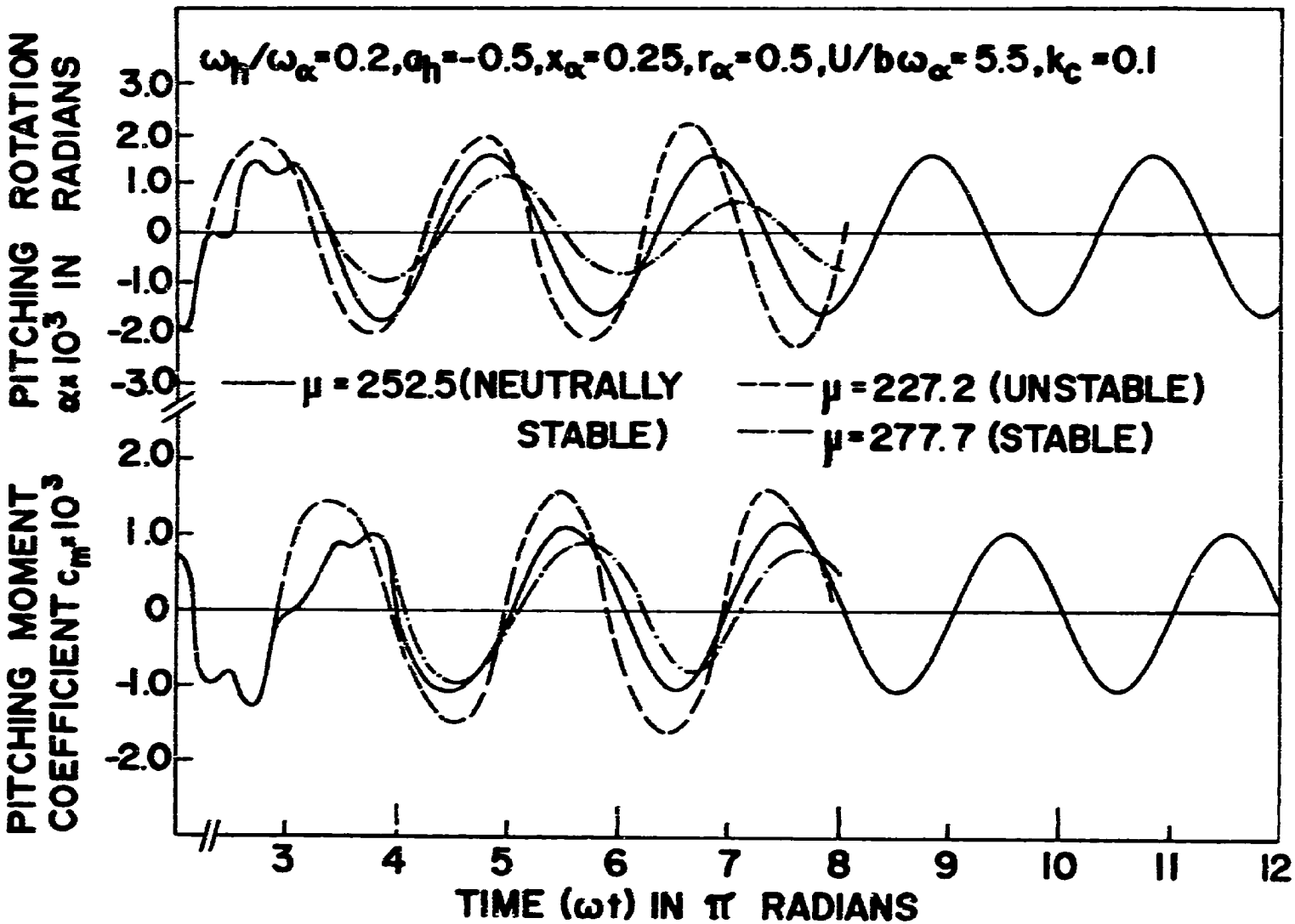

Figure 17. Effect of Airfoil-Air Mass Ratio (Altitude) on Pitching Rotation (α) and Pitching Moment (c_m) for NACA 64A006 Airfoil at M = 0.85.

method. On the other hand the flutter points predicted by the indicial and relaxation methods will result in a slightly diverging case.

The response results for the neutrally stable condition presented in Figures 16 and 17 also show the validity of the principle of superposition of air loads which was used in obtaining the flutter results by the U-g method. In deriving the equations for the simultaneous integration procedure it was not necessary to use such assumption.

In Figure 16, the response curves for plunging displacement ξ and lifting force c_ℓ for stable and unstable conditions are also shown. These were obtained by changing the airfoil-air mass ratio μ. For unstable response, the μ value assumed was 10% less than that corresponding to the neutrally stable condition. This point is in the unstable zone of Figure 15. On the other hand, for stable response the value of μ assumed was 10% higher than that corresponding to the neutrally stable condition. This point is in the stable zone of Figure 15. Stable and unstable response curves obtained for pitching displacement α and pitching moment c_m are also shown in Figure 17. It is seen that the stable and unstable conditions obtained by the U-g method produced converging and diverging responses, respectively.

It was also of interest to study the effect of airfoil-air mass ratio μ (altitude) on peak amplitudes of response curves. In this analysis, the peak amplitudes corresponding to the fourth cycle of free motion were considered. Figure 18 shows plots of the ratio of fourth cycle peak amplitude to the amplitude of the neutrally stable curves versus the ratio of airfoil-air mass ratio μ to the μ value corresponding to the neutrally stable point. These plots include four curves for plunging displacement, lifting force, pitching displacement and pitching moment, respectively.

From Figure 18 it may be observed that all the four curves have similar trends. The curve corresponding to pitching rotation is the steepest among the four curves. There is a sudden change in the slopes near the flutter point for all curves.

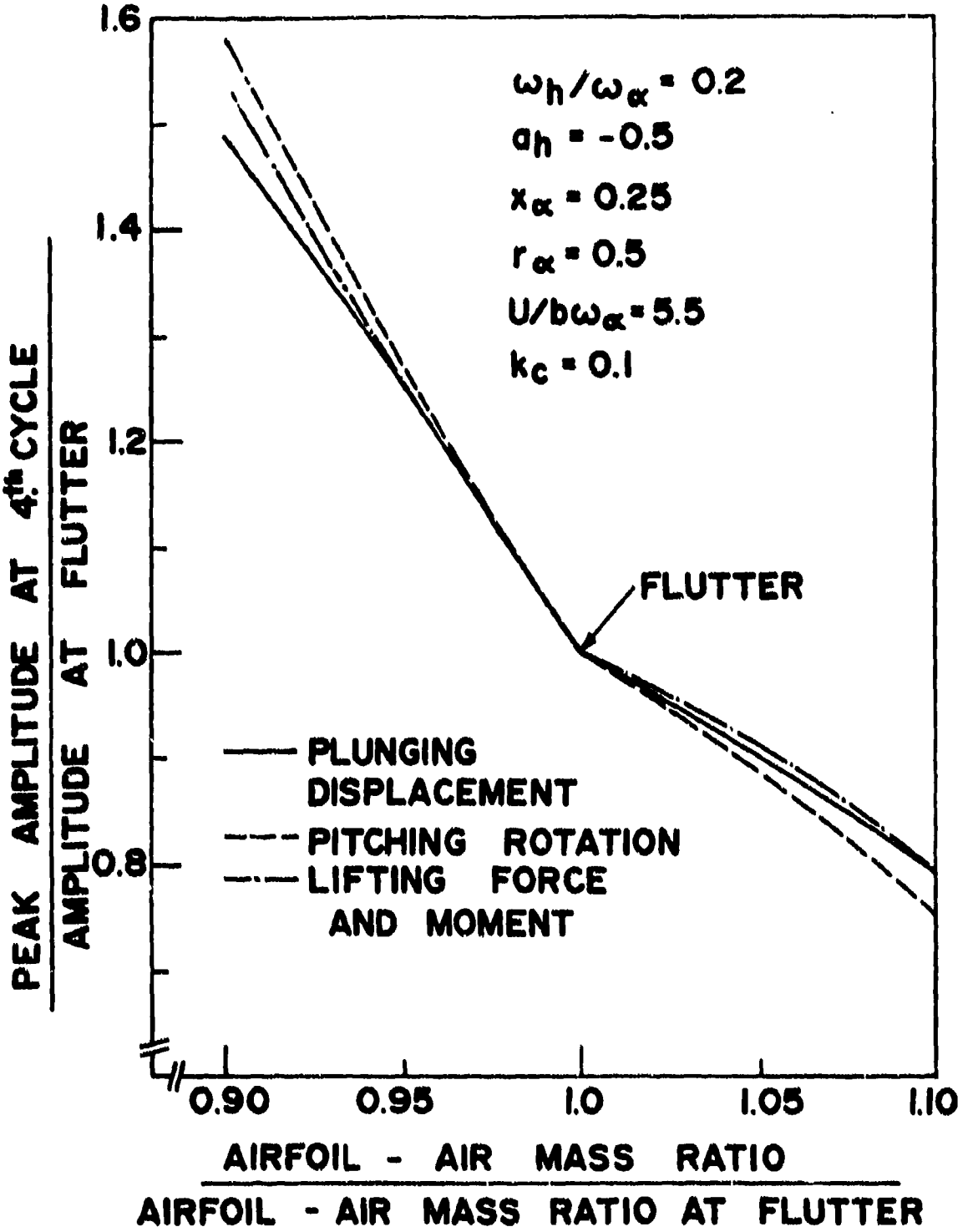

Figure 18. Effect of Airfoil-Air Mass Ratio on Peak Amplitudes of Responses for NACA 64A006 Airfoil at M = 0.85.

SECTION V

CONCLUDING REMARKS

The purpose of this research was to study the aeroelastic response behavior of single (plunging or pitching) and two degree of freedom airfoil systems in two-dimensional small-disturbance unsteady transonic flows. The aerodynamic computer code LTRAN2 which is based on a fully implicit finite difference scheme was employed to obtain the aerodynamic forces. Response behavior was studied for a flat plate at a subsonic Mach number of M = 0.7 and a NACA 64A006 airfoil at transonic Mach numbers 0.85 and 0.88. The influence of the airfoil-air mass ratio μ on response behaviors was studied in detail.

As a result of this study the following concluding remarks may be made:

(1) The response results obtained for single degree of freedom systems of pitching and plunging for flat plates at M = 0.7 show that LTRAN2 (linear) results compare well with the results based on quasi steady-state aerodynamic theory.

(2) Pitching response results obtained for a NACA 64A006 airfoil at M = 0.88 show that the present procedure of numerically integrating the structural and transonic aerodynamic equations gives results which agree with those obtained previously by Ballhaus and Goorjian (Reference 4).

(3) Results obtained for a flat plate with two degrees of freedom (pitching and plunging) at M = 0.7 illustrate that neutrally stable conditions obtained by the U-g method based on aerodynamic coefficients computed by the time integration method (LTRAN2) check with the neutrally stable conditions obtained by the time-response method. It was also illustrated that the neutrally stable conditions obtained by the U-g method based on aerodynamic coefficients obtained by the Kernel Function method compare well with those obtained by the time-response method.

(4) Response results obtained for a NACA 64A006 airfoil with two degrees of freedom (pitching and plunging) at the transonic Mach number M = 0.85 show that neutrally stable conditions obtained by the U-g method based on aerodynamic coefficients computed by the time integration method (LTRAN2) agree well with those obtained by the time integration response analysis. However, the neutrally stable conditions obtained by the U-g method based on the relaxation and indicial aerodynamic coefficients do not agree so well with that obtained by the time integration response analysis. This lack of good agreement may be due to the assumption of time linearization in the indicial and relaxation methods. Furthermore, the provision of treating the shock wave motion is lacking in the relaxation and the indicial programs.

(5) Good comparison between the neutrally stable conditions given by the U-g method (based on time integration aerodynamic coefficients) and the time-response analysis indicate that the principle of linear superposition of airloads used in the U-g method is valid for the cases analyzed.

(6) In general it may be concluded that the present method is accurate for predicting the neutrally stable conditions (flutter) for a two-degree-of-freedom system. This method also takes into consideration the movement of the shock whereas it is not possible to do so in the U-g method.

(7) Because of the limitations of the method employed in the computer code LTRAN2, only low reduced frequencies ($k_c < 0.2$) were considered in the analysis. Modifications to the LTRAN2 code are required for consideration of higher reduced frequencies.

(8) In this study it was also observed that M = 0.88 appears to be practically the highest Mach number that can be used in LTRAN2 for a NACA 64A006. Modifications in the basic code are required to account for higher Mach numbers.

(9) This analysis may provide a systematic procedure for the transonic aeroelastic response analysis of airfoils. The present study may also be used as a comparative basis by the experimentalists and other analysts who work in the same field.

(10) Similar studies on other airfoils, especially supercritical ones, are needed.

(11) In order to study more practical cases of full-wing aeroelastic responses, a transonic computer code to account for three dimensional unsteady flow is required.

REFERENCES

1. Bisplinghoff, R.L., Ashley, H., and Halfman, R.L., Aeroelasticity, Addison Wesley Publishing Company, Reading, Mass., 1955.

2. Yang, T.Y., Striz, A. G., and Guruswamy, P., "Flutter Analysis of Two-Dimensional and Two Degree of Freedom Airfoils in Small-Disturbance Unsteady Transonic Flow.", AFFDL-TR-78-202, AD A069223, December 1978.

3. Ashley, H., "On the Role of Shocks in the "Sub-Transonic" Flutter Phenomenon", AIAA/ASME/ASCE/AHS 20th Structures, Structural Dynamics, and Materials Conference, St. Louis, Mo., April 4-6, 1979.

4. Ballhaus, W.F., and Goorjian, P.M., "Computation of Unsteady Transonic Flows by the Indicial Method", AIAA Journal, Vol 16, No. 2, February 1978, pp. 117-124.

5. Rizzetta, D.P., "The Aeroelastic Analysis of a Two-Dimensional Airfoil in Transonic Flow", AFFDL-TR-77-126, December 1977.

6. Yang, T.Y., Guruswamy, P., and Striz, A.G., "Flutter Analysis of an NACA 64A006 Airfoil in Small Disturbance Transonic Flow" (to be published).

7. Traci, R.M., Albano, E.D., and Farr, J.L., "Small Disturbance Transonic Flows About Oscillating Airfoils and Planar Wings", AFFDL-TR-75-100, AD B008124L, June 1975.

8. Farmer, M.G. and Hanson, P.W., "Comparison of Supercritical and Conventional Wing Flutter Characteristics," Proceedings AIAA/ASME/SAE 17th Structures, Dynamics, and Materials Conference, King of Prussia, Pa., pp. 608-611, April 1976.

9. Rizzetta, D.P., "Transonic Flutter Analysis of a Two-Dimensional Airfoil", AFFDL-TM-75-168-FYS, May 1977.

10. Ballhaus, W.F. and Goorjian, P.M., "Implicit Finite Difference Computations of Unsteady Transonic Flows about Airfoils", AIAA Journal, Vol. 15, No.1, December, 1977, pp. 1728-1735.

11. Bathe, K.J. and Wilson, E.L., Numerical Methods in Finite Element Analysis, (chapters 8 and 9) Prentice-Hall, Inc., Englewood Cliffs, New Jersey 1976.

12. Olsen, J.J., "AGARD Standard Configurations for Aeroelastic Applications of Transonic Unsteady Aerodynamics, Part III, Candidate Airfoil Data", AFFDL-TM-78-6-FBR, Part III, January 1978.

13. Tijdeman, H. "Investigations of the Transonic Flow Around Oscillating Airfoils", National Aerospace Laboratory Report, NLR-TR-77090U The Netherlands, December 1977.

*U.S.Government Printing Office: 1979 — 657-002/69